Urban Water Research Association of Australia

New Concepts in Sludge Dewatering

Research Report No. 128

URBAN WATER RESEARCH ASSOCIATION OF AUSTRALIA (UWRAA)

The Association is a Division of the Water Services Association of Australia. UWRAA has the charter to develop and manage a portfolio of research to support the business plan for the urban water industry developed by the Water Services Association of Australia.

The UWRAA Research Report series presents information resulting from research projects supported by the Association and is published as a record of the work undertaken and as a means of disseminating the research findings. The Association also encourages the presentation of findings by the researchers in professional journals and at conferences. The Association's reports are indexed on STREAMLINE, the national water data base.

For further details contact:
Dr John Langford
Executive Director
Water Services Association of Australia
Level 7
469 Latrobe Street Telephone: (03) 9606 0678
Melbourne Vic 3000 Fax: (03) 9606 0376

Urban Water Research Association of Australia

New Concepts in Sludge Dewatering

P J Scales, S B Johnson, D Labbett,
University of Melbourne

D R Dixon, CSIRO Division of Chemicals and Polymers

Research Report No 120
May 1997

ISBN 1 876088 26 5

FOREWORD

This report is based on UWRAA Research Project No SS 59: 'New Concepts in Sludge Dewatering' which was undertaken during the period February 1994 - February 1996. Organisational resposibility for the project was as follows:

Sponsoring Authority:	Brisbane City Council
Research Agencies:	Advanced Mineral Products Special Research Centre, School of Chemistry, University of Melbourne, Parkville, Victoria
	CSIRO, Division of Chemicals and Polymers, Clayton, Victoria
Project Officer:	Mr Mark Pascoe Brisbane City Council (now employed at Woodward Clyde, Milton, QLD)
Principal Researcher:	Dr Peter J Scales Advanced Mineral Products Special Research Centre, School of Chemistry, University of Melbourne.

The project was funded by the Urban Water Research Association of Australia.

SYNOPSIS

The inter-relationship between the addition of chemicals in the clarification of potable water and the volume and ease of dewatering of the subsequent sludge is poorly understood and indeed, poorly quantified. Current operating practices have been reviewed and the application of the most recent theories of the compressional dewatering of sludges has been considered for potable water (nominally alum) sludges. This involved laboratory, pilot plant and full scale tests.

Quantitative laboratory characterisation methods for the compressibility (extent of dewatering) of sludges have been available for a number of years along with other methods for characterising the permeability of sludges (rate of dewatering). Sludges such as those typical of alum flocculated potable water sludges are usually of low volume fraction solids and even after clarification and centrifugation, the increase in solids of these sludges is not extensive, despite a residual cake that has no apparent free water. It is the inter-relationship between the solids content of the cake, the energy required to achieve this condition with typical dewatering equipment and the type and quantity of chemicals present that was of interest to this study.

The compressibility of real and model alum coagulated sludges was examined using a laboratory based centrifugation technique in the presence of a range of polymeric additives to gauge the absolute dewaterability of the sludges. This proved useful in scaling the effectiveness of equipment currently utilised in the industry. The role of alum in controlling the dewatering process was examined in detail. The role of dispersant style chemical additives on reducing the effect of the alum was also examined. Tests were performed at a laboratory, pilot and full scale.

The key conclusions of the study relate to the role of the large doses of alum characteristically used in water treatment in controlling the rigidity of water treatment sludges. The control renders polymeric additives used in secondary concentration processes such as thickening and centrifugation ineffective. Recommendations are made as to the optimisation of sludge handling procedures and equipment.

TABLE OF CONTENTS

INTRODUCTION

The concentration of fine particles from low solids slurry wastes is of importance to many minerals-based industries. Such 'dewatering' technology commonly forms the basis for possible regeneration of water while providing a high solids loading product for recycle or disposal. This waste sludge is sometimes treated for recovery of valuable components and/or transported for final disposal as landfill.

Largely economic concerns over the cost of both transportation and storage of waste solids have in recent times led to a heightened interest in dewatering optimisation within the Australian potable water industry. In particular, attention has been focused on regions where the raw water supply is highly turbid, leading to relatively large volumes of waste slurry requiring disposal. The Brisbane river, providing water to Brisbane and surrounding shires, is such an example.

The use of coagulants such as aluminium sulphate (alum) to clarify water and the subsequent use of high molecular weight (MW) polyelectrolyte style flocculants in the sludge dewatering processes is well established. These mechanisms are the basis for the potable water production process at Brisbane City Council's Mount Crosby Westbank Water Treatment Plant, near Brisbane, from which waste treatment sludge was obtained for use in this study.

Assuming that the coagulant dose is optimised, initial treatment of raw water with alum provides rapid clarification while providing a gelatinous waste that typically settles to *ca.* 1.2 to 2.5 weight percent (w/w %) solids. Treatment of this waste with high MW polyelectrolyte again provides rapid supernatant clarification, while producing a filterable product that will typically consolidate to *ca.* 15 to 20 w/w % solids under the artificial gravimetric conditions imposed by high speed centrifugation.

It has recently been theorised that rapid methods of particle destabilization in solution using ionic coagulants and high MW polyelectrolytes may be inherently detrimental to the extent of final waste sludge dewaterability [1]. The authors postulate an intimate link between the

compressibility (extent of dewatering) of flocculated suspensions and the mechanism of flocculation.

The aim of this work was to closely examine the methods of waste solids flocculation and dewatering currently practiced in the Australian water industry to elucidate the effectiveness of these operations, as judged by recently developed theoretical methods for examining the compressibility/filterability of particulate slurries[2, 3]. An additional aim was to examine the use of low MW surface-adsorbed molecules in the dewatering process. Such molecules have been demonstrated to have a dramatic effect in the dispersion of difficult to compress particulate fluids in selected laboratory systems[4, 5]. This provides the possibility of achieving a final sludge product of substantially increased solids content.

Laboratory work described in this report was performed at the University of Melbourne and at Mount Crosby Westbank Water Treatment Plant near Brisbane. Pilot and full scale tests were performed at the Mount Crosby Westbank Water Treatment Plant.

CONSOLIDATION OF COLLOIDAL SUSPENSIONS

It is well established that, if allowed to settle under gravitational or centrifugal forces, a non-aggregated aqueous particle suspension will form a high solids deposit at the base of the vessel. However, the finely dispersed nature of many natural suspensions makes the time domain over which this process will occur far too great for practical industrial application. As a consequence, ionic and high molecular weight polymeric flocculants are commonly added in order to induce aggregated particle sedimentation. The resulting floc structures settle quickly due to their relatively high mass to surface area ratio. An open network sediment bed of flocs is rapidly formed. This network is of lower average volume fraction than would be the case if non-aggregated settling was to occur.

Although seemingly flimsy, the floc sediment network can take on some solid-like properties, in particular the ability to resist compressive stresses such as are supplied by a centrifuge or a

filter or more simply by the weight of particles in the bed of a clarifier or thickener. The compressive stresses are resisted up to a compressive yield stress, beyond which the network will irreversibly deform. Buscall and White[2] have defined a concentration dependent yield stress, $P_y(\phi)$, beyond which flocculated suspensions at volume fraction ϕ will no longer resist compression. The form of the compressive yield stress as a function of solids volume fraction is shown in Figure 1.

In the Buscall and White model, $P_y(\phi)$ is defined as dependent upon the balance of three forces, these being the gravitational driving force of compression, the hydrodynamic drag due to liquid flow out of the network, and the elastic particle stress caused by particle-particle interactions. While the gravitational and liquid viscous drag parameters are of obvious importance in development of dewatering technology, it is the changes in $P_y(\phi)$ induced through manipulation of critical particle-particle interactions that are primarily of interest in this study. In summary, the main question of interest is, can we manipulate the elastic particle stress component resulting from the interaction between particles by changing the chemistry of the coagulation/flocculation process and so enhance dewatering?

The flocculation and clarification process is driven by the destabilisation of suspension particle-particle interactions. In the context of this report, the word stabilisation refers to the ability of particles to resist coagulation. In reducing the stability of the final floc sediment (ie. decreasing the attractive interaction between particles), a lower compressive pressure is required to reach a desired volume fraction. In practical terms, a higher sludge solids content is attainable. A number of distinct mechanisms are currently believed to cause particle destabilisation in colloidal suspensions [1, 6]. These include:

(a) compression of the electrical double layer (see forthcoming text).
(b) flocculant adsorption to produce charge neutralisation.
(c) enmeshment in precipitate, the so-called "sweep coagulation" process.
(d) inter-particle polymeric bridging induced by flocculant adsorption.
(e) surface adsorption of specific low MW molecules to sterically hinder coagulation processes.

The use of alum as an ionic coagulant has been extensively studied with respect to potable water production. The coagulation processes initiated by alum depend critically upon the dosage applied, with surface charge neutralisation resulting with application of a relatively low alum concentration. Sweep coagulation arises with use of more substantial alum dosages. Chemical interactions occurring during both processes are depicted schematically in Figure 2 (after Amirtharajah[7]). As shown, the cationic products of the alum hydrolysis reaction must interact with the negatively charged colloids typically present in the raw water in order for particle destabilisation to occur [8].

The primary mechanisms of action when organic polyelectrolytes are used in the flocculation process are considered to be inter-particle bridging and surface charge neutralisation, the latter mechanism dependent upon the charge characteristics of the polyelectrolyte utilised. The use of relatively low MW hydrophilic molecules, such as citrate, malate and lactate in an effort to destabilize the alum floc structure is a concept which will be developed in this report. The use of such molecules is aimed at decreasing particle-particle interaction and in some way modulating the effects of added alum and polyelectrolytes.

Obtaining the desired compressibility, clarification and dewatering properties for a given system may involve simultaneous use of a number of flocculants with differing mechanisms of action. In short, such methods of optimising flocculant properties and use for both water clarification and for sludge dewatering were of interest to this study.

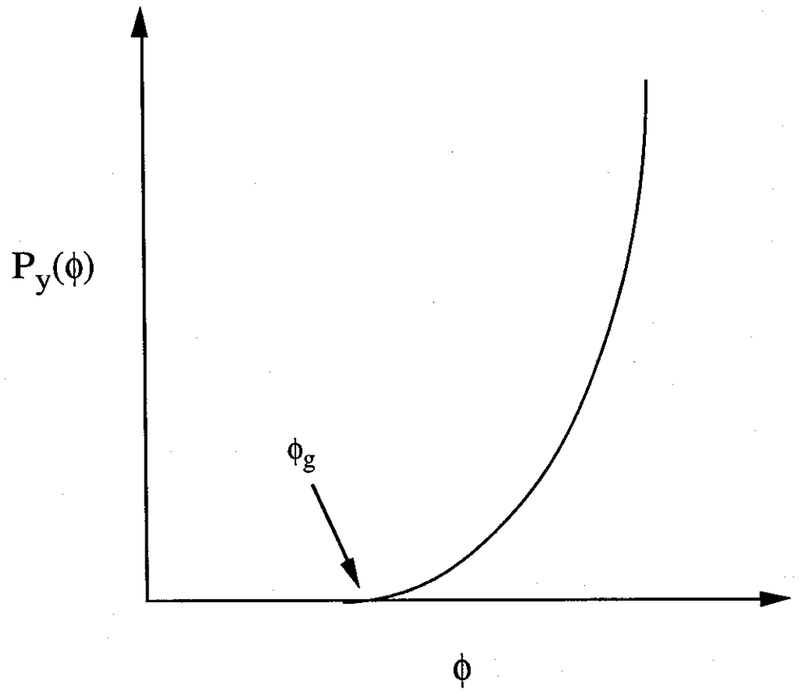

Figure 1 Variation of the compressive yield stress, $P_y(\phi)$, as a function of solids volume fraction, ϕ, according to the Buscall - White theory [2]. The point labelled ϕ_g is referred to as the gel point, beyond which the compressive yield stress is non-zero and an applied force is required to dewater the solid suspension.

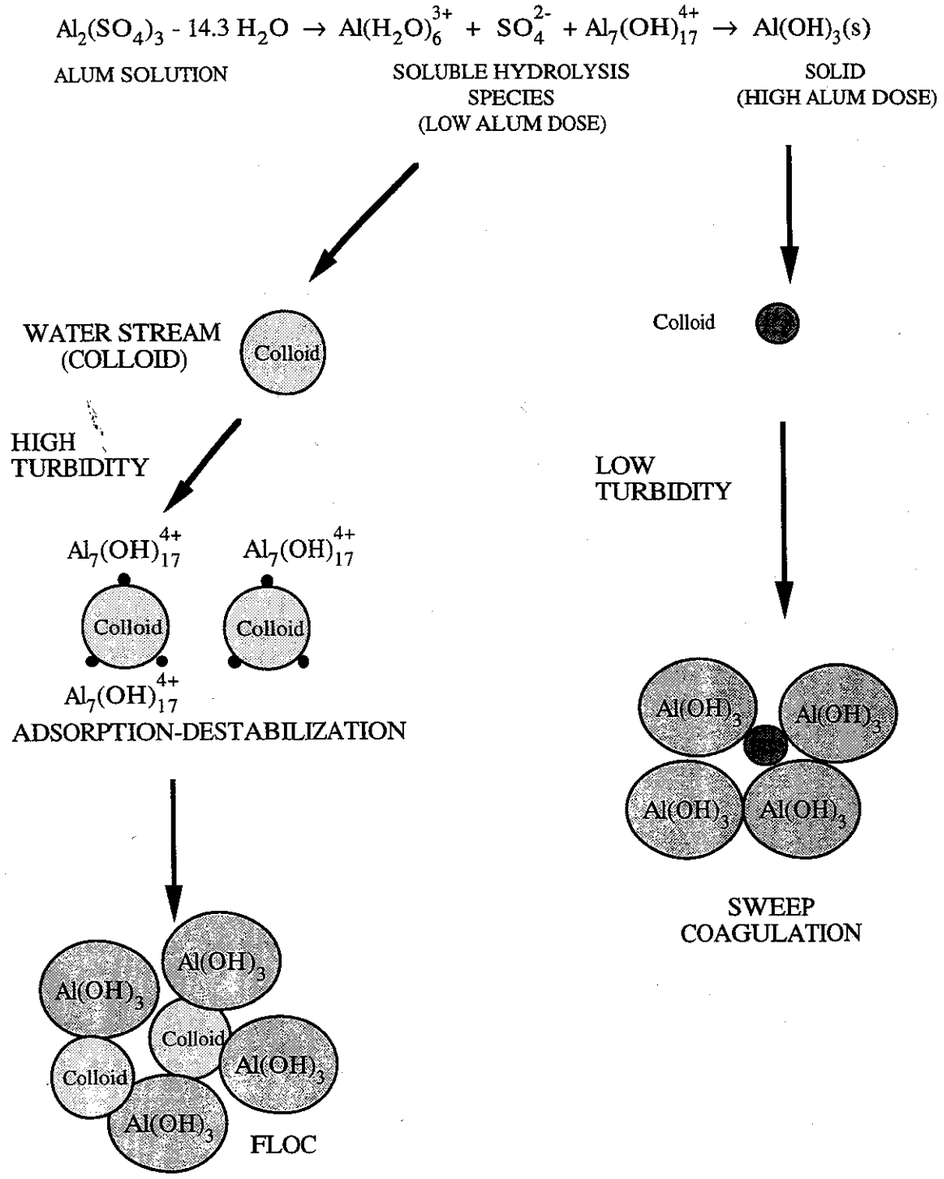

Figure 2 Overview of chemical interactions taking place during the potable water purification process initiated by alum, $Al_2(SO_4)_3$ (after Amirtharajah [7]).

ELECTROKINETIC CHARACTERISATION OF COLLOIDAL SUSPENSIONS

The Electrical Double Layer

When a colloidal particle is brought into contact with an aqueous electrolyte medium, the net orientation of water molecule dipoles at the resulting interface promotes electrical charging of the colloid surface. Usual mechanisms for this process include ionisation of surface sites and ion adsorption from solution. The combination of the charged interface and an unequal distribution of counter-ions over co-ions in the surrounding aqueous environment is commonly referred to as the electrical double layer, an understanding of which is essential to the prediction of the flocculation and dewatering properties of charged colloidal systems. An idealized view of the electrical double layer is shown in Figure 3.

If a liquid is flowed relative to a charged solid, Helmholtz in 1879 recognised that solvated molecules comprising a compact inner double layer would remain adsorbed to the solid surface. For this reason, the concept of a hydrodynamic surface of shear was developed, this being an electrical double layer plane within which infinite solvent viscosity is assumed. The average potential in the surface of shear is defined as the zeta potential, or ζ [9]. The zeta potential is a prime determinant of the interaction energy between particles and hence the compressibility and ultimate dewaterability of a particulate suspension.

Experimental determination of the zeta potential may be achieved through manipulation of electrokinetic phenomena such electrophoresis, streaming potential, electro-osmosis and the sedimentation potential. Each of these techniques measures the displacement of a charged colloidal particle or surface relative to the surrounding aqueous phase, and is limited to examination of a relatively small number of individual entities. Electroacoustics is a more recent electrokinetic innovation, which, unlike the more traditional electrokinetic techniques, has the advantage of being able to characterise concentrated colloidal samples. It was therefore considered ideal for electrokinetic examination of the waste potable water sludges of interest in this study.

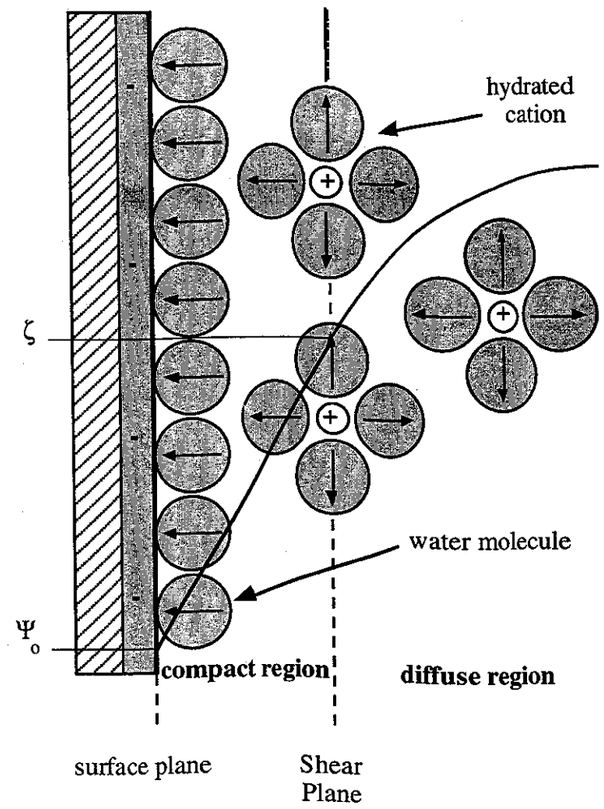

Figure 3 An overview of the electrical double layer at the surface of a charged particle. ψ_0 represents the colloidal surface potential and ζ is the shear plane or zeta potential.

Electroacoustic Determination of the Zeta Potential

The generation of an alternating electric field by a sound wave as it passed through an electrolyte medium was first predicted by Debye [10]. This effect was also presumed to occur for suspended colloidal suspensions, and was termed the Colloid Vibration Potential, or CVP [11]. The discovery of the converse phenomenon, whereby sound waves are generated by an applied electric field was made in 1985 [12]. This effect was termed the Electrokinetic Sonic Amplitude, or ESA. When an alternating voltage is applied to a colloidal suspension, the particles oscillate at a velocity that is dependent upon their size and zeta potential. Provided that the particles are of a different density to the aqueous medium, pressure forces arise at the suspension boundaries, propagating as sound waves back into the suspension and through the material/s comprising the boundaries.

The Acoustosizer instrument (Matec Applied Sciences) utilises two parallel plate electrodes embedded in the walls of a sample cell for the generation of a pulsed alternating electric field perpendicular to the electrodes [13]. The electrodes are attached to a pair of glass rods. Generated sound waves propagate down the glass rods, and are detected by the transducer attached to the end of the right hand block (Figure 4). The glass rods serve to delay sufficiently the arrival of the signal at the transducer that it can be differentiated from unwanted electrical "cross talk" generated by the application of the high voltage pulse across the cell. The Acoustosizer varies the applied voltage pulses over thirteen discrete frequencies ranging from 300 kHz to 11 MHz, thus generating an ESA spectrum for the suspension.

For an isotropic concentrated colloidal suspension, the ESA signal may be related to the particle-averaged dynamic mobility, $\langle \mu_D \rangle$, by the expression [14]

$$ESA = A\phi\frac{\Delta\rho}{\rho} < \mu_D > \frac{E}{S_A - S_S} \qquad (1)$$

where A is an instrument constant dependent on the properties of the detecting transducer and the signal processing electronics, ϕ is the particle volume fraction, ρ is the liquid density, $\Delta\rho$ is the density difference between the solid and liquid phases, and E is the magnitude of the applied

field. Determination of the quantities S_A and S_S is performed by reapplying the alternating voltage pulse across the transducer on the left-hand glass rod depicted in Figure 4. This generates a sound wave that travels down the rod and is partially reflected at the rod-particle suspension interface. S_A and S_S are then calculated as the Fourier Transforms of the partially reflected signals from the transducer in the presence of air and the particle suspension respectively.

For a spherical particle with a thin double layer, the dynamic mobility is related to ζ and spherical-equivalent particle radius, a, by the expression [15]

$$\mu_D = \frac{\varepsilon\zeta}{\eta} G(\alpha) \qquad (2)$$

where η is the viscosity and ε is the permittivity of the liquid. $G(\alpha)$ is best described as an inertial term. Fitting the frequency response of the magnitude and phase of $\langle\mu_D\rangle$ allows us to predict both the particle size and zeta potential for a particle suspension.

The measurement and zeta potential determination are controlled within the Acoustosizer software.

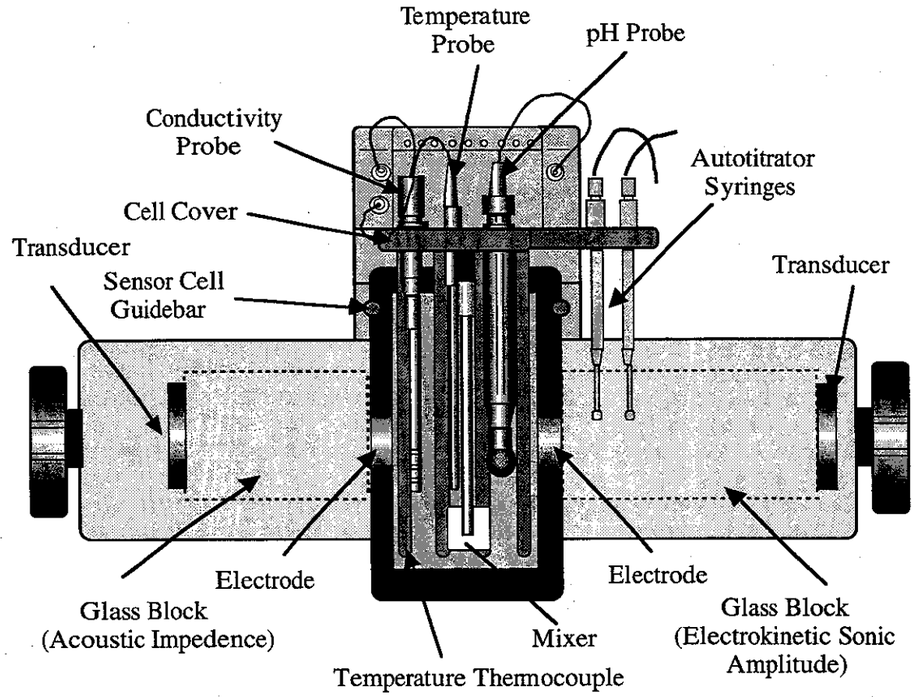

Figure 4 The measuring cell of the Acoustosizer instrument (Matec Applied Sciences). Attachments allow the solution temperature to be controlled, solution pH and conductivity to be monitored, and auto-titration of the sample.

RHEOLOGICAL CHARACTERISATION OF COLLOIDAL SUSPENSIONS

Changes in the surface properties of a colloidal particle will inevitably exacerbate themselves in concentrated colloidal suspensions as alterations in the rheological properties of the system. This has implications for both shear and compressive behaviour of concentrated colloidal suspensions. Therefore, monitoring the shear and compressive rheology of a colloidal suspension provides a method by which the bulk mechanical properties of a suspension may be linked to particle surface properties and hence to dewatering processes.

Determination of the Shear Yield Stress

Most interest in determination of the shear yield stress comes from the need to characterise the flow properties of colloidal suspensions. Such studies have obvious implications for the processing (ie. pumping and flow behaviour) of industrially important particulate suspensions. While rotational viscometers have traditionally been used in direct shear yield stress determination, problems have arisen due to the phenomenon of wall slip inherent in these techniques and the need to extrapolate data to a zero shear condition to obtain a yield stress. In order to avoid such pitfalls, the single point vane technique of Nguyen and Boger [16] was utilised in this study. This method uses a slowly rotating four bladed vane immersed in the sample. The applied torque is monitored as the vane rotates, with the yield stress being calculated from the maximum observed torque. The shear yield stress, as measured, is best visualised as the minimum force required to initiate flow in a yielding suspension. All self supporting particulate networks such as are typical of alum rich potable water sludges have a finite shear yield stress.

Calculation of the shear yield stress, τ_y, requires knowledge of the geometry of the vane and the stress distribution over the cylindrical sample yielding surface. It can be shown that the torque, F, applied to the shaft is given by the relation [16]

$$F = \left(2\pi R_v H_v\right) \tau_w R_v + 2\left(2\pi \int_0^{R_v} \tau_e(r) r^2 dr\right) \qquad (3)$$

where R_v and H_v are the radius and height of the vane respectively, τ_w is the shear stress at the cylinder wall and $\tau_e(r)$ is the shear stress distribution on the ends of the cylinder. At the moment of yielding, $\tau_w = \tau_e = \tau_y$ and F is at a maximum, F_{max}. For vanes of relatively small diameter, D_v, it may be assumed that shear stresses are uniformly distributed at the ends of the cylinder such that $\tau_e(r) = \tau_w$. Also assuming that the sample yields instantaneously along the cylindrical surface, equation 3 may be simplified to [17]

$$F_{max} = \frac{\pi D_v^3}{2}\left(\frac{H_v}{D_v} + \frac{1}{3}\right)\tau_y \qquad (4)$$

Equation 4 enables a single point measurement of the shear yield stress. In the present study, a Haake RV3 vane viscometer as shown in Figure 5 was utilised. A number of vanes of differing dimensions were available, enabling accurate torque readings over a wide range of suspension conditions.

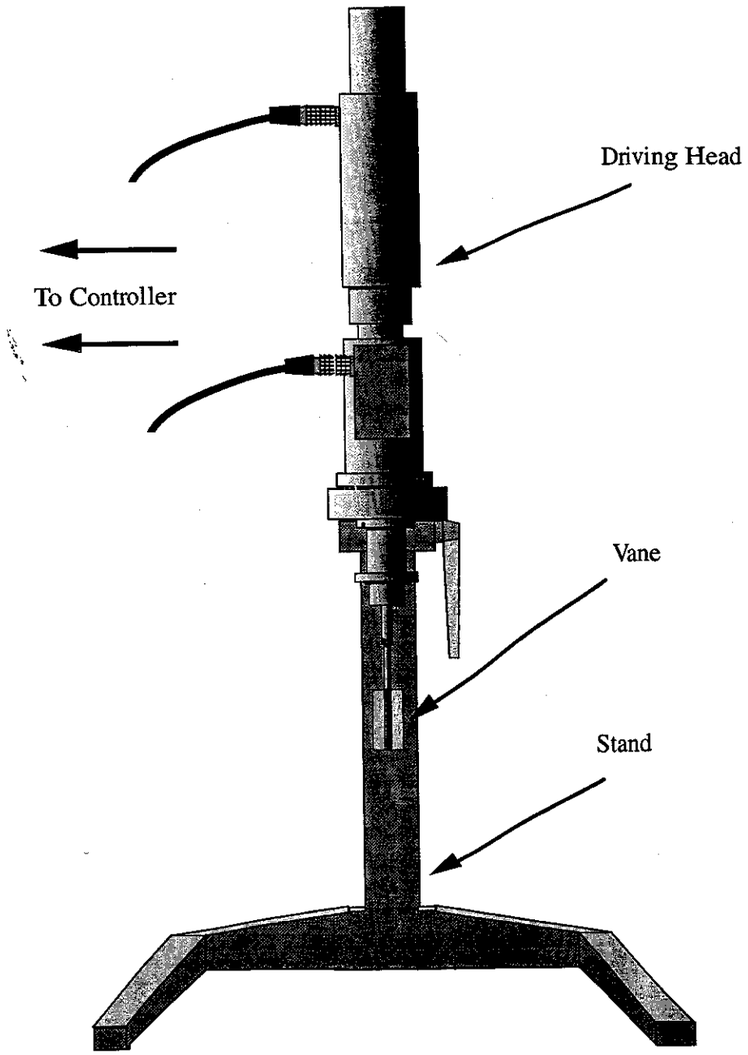

Figure 5 The Haake RV3 vane viscometer used in determination of the shear yield stress.

Determination of the Compressive Yield Stress

The obvious importance of laboratory compressive yield stress determination lies in its ability to predict colloidal consolidation (dewatering) properties in industrial thickening, filtration and centrifugation devices while operating on a much smaller and more economically desirable scale. Traditional theories of compression have often relied upon the fitting of experimental data to yield an empirical relationship, or required estimations of unmeasurable parameters needed in the modelling.

The use of swinging-bucket centrifuges in simulation of compressive forces was first proposed by Lockyear and White [18] and later developed by Buscall and White [2]. The Buscall and White model is based upon a process of measuring the equilibrium sediment height, H_{eq}, as a function of the gravitational field at the base of the bed, g, where the initial sediment height, H_0, and solids volume fraction, ϕ_0, are known. Solving the equations derived is mathematically complex, requiring a lengthy iterative process. However, approximations to the exact solution are available. In the present study, a mean value theorem refined by Green et al. [19] was utilised in calculation of the compressive yield stress, $P_y(\phi)$, yielding the expressions

$$P_y(\phi) = \Delta\rho g \phi_0 H_0 \left(1 - \frac{H_{eq}}{2R}\right) \text{ and} \tag{5}$$

$$\phi = \frac{\phi_0 H_0 \left[1 - \frac{1}{2R}\left(H_{eq} + g\frac{dH_{eq}}{dg}\right)\right]}{\left[\left(H_{eq} + g\frac{dH_{eq}}{dg}\right)\left(1 - \frac{H_{eq}}{R}\right) + \frac{H_{eq}^2}{2R}\right]} \tag{6}$$

where $\Delta\rho$ is the density difference between the liquid and solid phases, and R is the radius of the centrifuge at the consolidation bed base.

In this study, a Beckmann GS-15R bench-top centrifuge was utilised with operating speeds between 300 and 1700 rpm. Samples were maintained at *ca.* 5°C to inhibit both rapid polymer degradation and sample bio-activity.

ALUM FLOCCULATION PROCESSES

Sweep flocculation of particulate matter from raw water with metal hydroxides is the basis of rapid water clarification in many parts of Australia and around the world. This is the case at the Mount Crosby Westbank Water Treatment Plant, near Brisbane. The process begins with addition of aluminium sulphate (alum) to the incoming raw water, forming a hydrous gel that traps unwanted particulate and organic matter (Figure 6). The combined waste gradually settles as the water passes down sedimentation basins, and is periodically removed using mobile bridges incorporating submersible pumps. The chemically flocculated and settled water then passes into Dissolved Air Flotation (DAF) chambers, where pressurised streams of air saturated water are injected, inducing a rapid formation of very fine air bubbles. These return to the chamber surface, floating residual floc particles to the surface. The sludge forms a stable surface sludge which is regularly removed by hydraulic means. Finally, purified water is passed through a series of sand/gravel filters before undergoing standard chloramine disinfection and addition of lime for pH correction.

To prevent blockage, the sand/gravel filters are cleaned by daily backwashing, providing a further source of waste aqueous slurry. Waste sludge obtained from alum flocculation, DAF treatment and sand/gravel filter backwashing is combined in a holding tank, providing a suspension of *ca.* 0.1 weight percent (w/w %) solids for treatment.

The use of sweep flocculation as the primary process for water purification provides a rapid method of supernatant clarification. Clarification time is found to decrease rapidly as alum dosage is raised [20]. On the down side, the sweep flocculation process often requires large quantities of alum. This is not only economically undesirable, but creates an excess of waste sludge. Significantly, the extent of dewaterability of the sludge is known to decrease as suspension alum concentrations rise [20, 21]. As mentioned previously, there exists a trade-off between the rate of flocculation and the extent of dewaterability.

In the following work, the use of alum as a flocculant has been studied with respect to its effects on the surface properties of sludges as a function of concentration. Due to the large

volumes of water required to generate a workable quantity of raw sludge and the draw backs of using untested alum doses on a full plant scale, model sludge systems have been utilised in approximately half of the laboratory work. The make-up of model sludges was based on elemental analysis of several plant sludge samples and a typical result for a Mount Crosby sedimentation sludge showed the sludge to be ≈30 w/w % aluminium hydroxide, 30 w/w % humics (organic matter) and 40 w/w % silicates and clays.

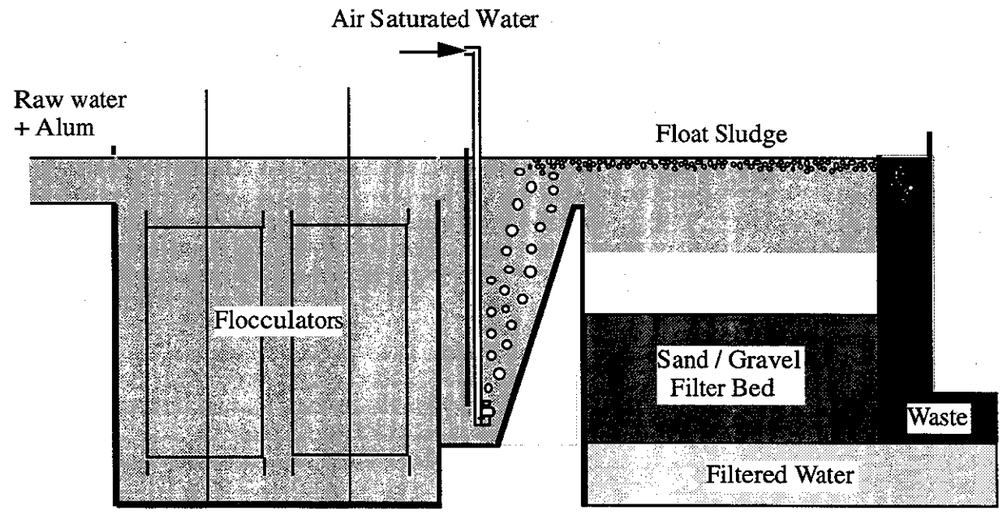

Figure 6 The potable water alum sweep flocculation process as used at the Mount Crosby Westbank Water Treatment Plant, near Brisbane.

Experimental Section

Initial studies involved characterisation of an alumina system in the presence of 10^{-3} mol dm^{-3} background NaCl. The alumina (high purity AKP-30: Sumitomo Chemicals) was almost monodisperse, non-porous and spherical, providing an ideal model system for study.

Simplified model sludges were made up of clay (kaolinite), 10^{-3} mol dm^{-3} background NaCl, and varying doses of aluminium, in the form of $AlCl_3$. Crude kaolinite was obtained from Weipa, Queensland. It was prepared by dispersion with a small amount of sodium metaphosphate (Calgon T: Ajax Chemicals) and high speed blunging at 45 w/w % solids. The kaolinite dispersion was passed twice through a high gradient magnetic separator (Eriez Magnetics) at *ca.* 1.7 Tesla in order to remove iron impurities. It was finally dialysed until the conductivity approached that of Milli-Q water (conductivity < $1x10^{-6}$ Ω^{-1} cm^{-1} at 20°C) and dried at *ca.* 40°C. $AlCl_3$ and NaCl were analytical grade reagents.

Further model sludges were prepared to examine the significance of organic materials such as humics and fulvics on the suspension surface properties. In this case, humic acid (Na salt, technical grade: Aldrich Chemicals) was used as the source of organics. Due to the lengthy preparation time required to obtain only small amounts of kaolinite, silica (laboratory grade: Sigma Chemicals) was also used. This was considered acceptable as kaolinite surface chemistry is dominated by its negative silica-like face. Model sludges were made from silica and humic acid in the proportion 100:1, substantially below the organic contribution to natural waters. This was due to the far greater solubility of the humic acids relative to that of raw water organics. The dosage of alum was again varied. All samples were prepared at pH 5.5, close to that found in natural waters, although water from the Brisbane River has a higher pH.

Electrokinetic and rheological measurements were made using the electroacoustic and shear yield stress instruments. The pH was altered using analytical grade HCl and NaOH. Apparent colour was measured via absorbance measurements with reference to a standard Pt - Co calibration curve. Absorbance experiments were performed on a Hitachi U-2000

Spectrophotometer at a wavelength of 400 nm. Turbidity measurements were performed on a Hach Ratio Turbidimeter.

Results and Discussion

Model Alumina System

The electrokinetic properties of high purity alumina in the presence of 10^{-3}M NaCl background electrolyte are shown in Figure 7. The zeta potential is seen to be positive at low pH, and gradually decreases as the pH is increased. The point of zero charge (pzc) occurs at pH 9.1. The shear yield stress obtained under identical background conditions is shown as a function of both pH and volume fraction in Figure 8. In all cases, no yield stress was detectable below pH $\approx$ 7.3 or above pH $\approx$ 11.2. The maximum shear yield stress occurs at pH $\approx$ 8.8, in reasonable accordance with the electrokinetic pzc. The flocculation point, based on a non-zero value for the yield stress, occurs at a ζ magnitude of 38 mV. The behaviour was found to be symmetrical about the pzc. The flocculation/dispersion points are also indicated in Figure 7.

Kaolinite and Aluminium Flocculated Systems

Figure 9 shows the shear yield stress of the Weipa purified kaolinite in 10^{-3}M background electrolyte as a function of both pH and volume fraction. In all cases, the yield stress is seen to rise to a maximum at pH $\approx$ 5.0 to 5.5 and then decreases. There is no discernible yield stress beyond pH $\approx$ 11.2. Kaolinite surface chemistry is known to be dominated by interactions between the positive aluminium dominated edges and the negative silica dominated faces.

These interactions vary across the pH range, as shown schematically in Figure 10. As labelled, at pH values less than A, edge-face hetero-coagulation and face-face coagulation is dominant, between A and B, the suspension assumes a "house of cards" type structure due to edge-face hetero-coagulation [22]. This structure gradually breaks down as pH rises, and between B and C, both edge-face and edge-edge attraction occurs. Between C and D, only edge-edge coagulation is predicted, with dispersion occurring beyond this point. In this case, D corresponds with the pH of zero yield stress at pH $\approx$ 11.2.

In practice, as the surface area of the kaolinite face far exceeds that of the edge, the surface chemistry is expected to be dominated by the face interactions unless the face is otherwise neutralised. The kaolinite electrokinetic potential as a function of pH is shown in Figure 11. In the absence of aluminium addition, the ζ-potential is indeed found to follow a form consistent with the face potential. As $AlCl_3$ is added, ζ gradually rises across the pH range and become more consistent with aluminium-type potentials, as previously shown in Figure 7. This is presumably due to the Al^{3+} binding with and neutralising the negative faces, leaving both positive edges and free hydrous aluminium in solution to control the surface chemistry of the system. The shear yield stress of kaolinite suspensions as a function of $AlCl_3$ concentration is shown in Figure 12. As the dose of $AlCl_3$ rises, the shear yield stress curves become a distinct mixture of kaolinite and aluminium properties. By the point that the $AlCl_3$ dose reaches 25 dry weight based percent (dwb%) on solids, the shear yield stress is representative of typical aluminium-type behaviour. A parabolic curve is obtained, with the maximum yield stress at pH ≈ 8.7 in good agreement with the aluminium electrokinetic pzc (Figure 7).

Figures 13 and 14 show the effect of several different counter-ions upon the electrokinetic and shear yield stress properties respectively of an aluminium flocculated kaolinite system. In both cases, changes in counter-ion produced only a slight difference in the data, presumably related to differences in the bulk solution conductivities. On this basis, the experimental interchange of $AlCl_3$ for alum appears reasonable.

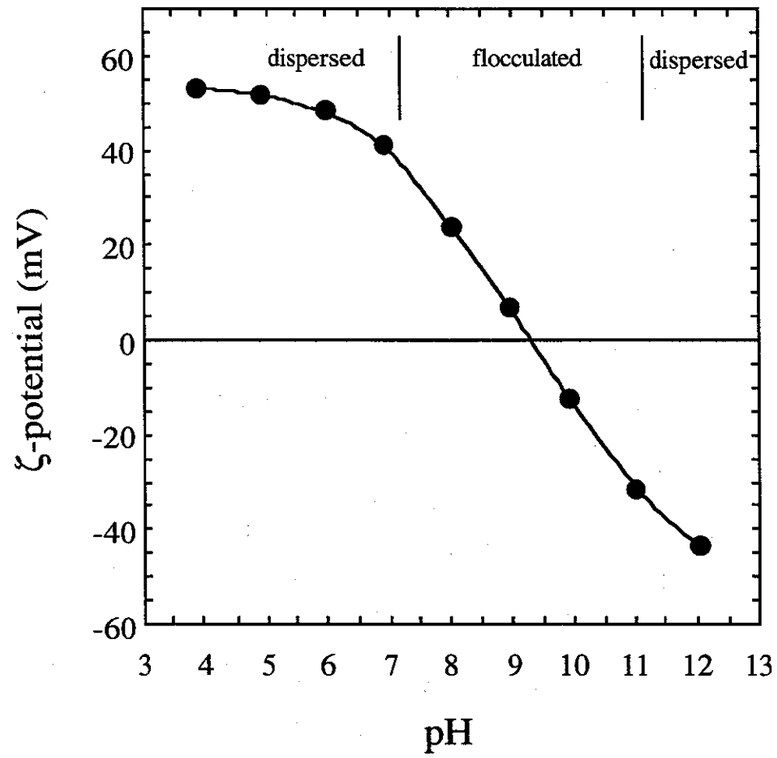

Figure 7 The electrokinetic ζ-potential as a function of pH for a 2.0 volume percent (v/v %) AKP-30 high purity alumina / 10^{-3} mol dm^{-3} NaCl model system. The point of zero charge (pzc) of the particle surface is indicated, as are the expected limits of particle dispersion.

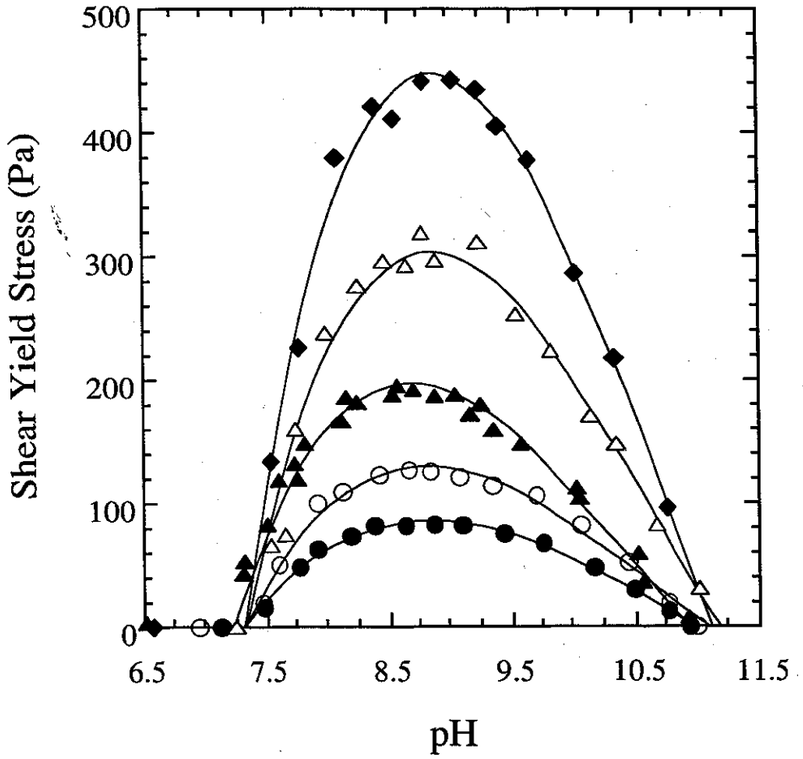

Figure 8 The shear yield stress as a function of both volume fraction and pH for a AKP-30 high purity alumina / 10^{-3} mol dm^{-3} NaCl model system. ● = 20.0 v/v % alumina; ○ = 22.5 v/v %; ▲ = 25.0 v/v %; △ = 27.5 v/v %; ◆ = 30.0 v/v %.

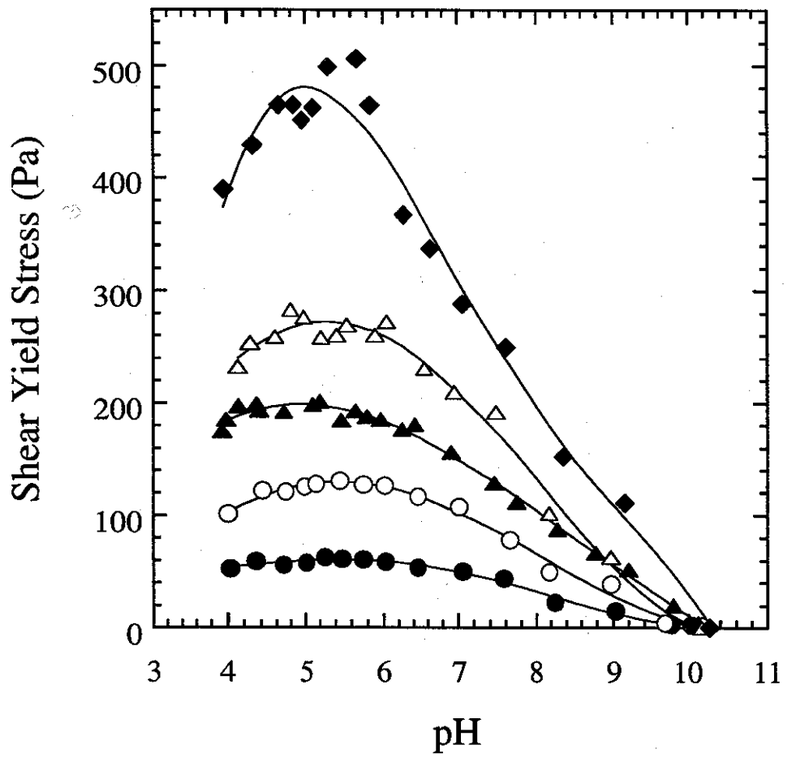

Figure 9 The shear yield stress as a function of both volume fraction and pH for a purified Weipa kaolinite / 10^{-3} mol dm^{-3} NaCl model system. ● = 9.8 v/v % kaolinite; ○ = 12.3 v/v %; ▲ = 13.8 v/v %; △ = 14.8 v/v %; ◆ = 17.3 v/v%.

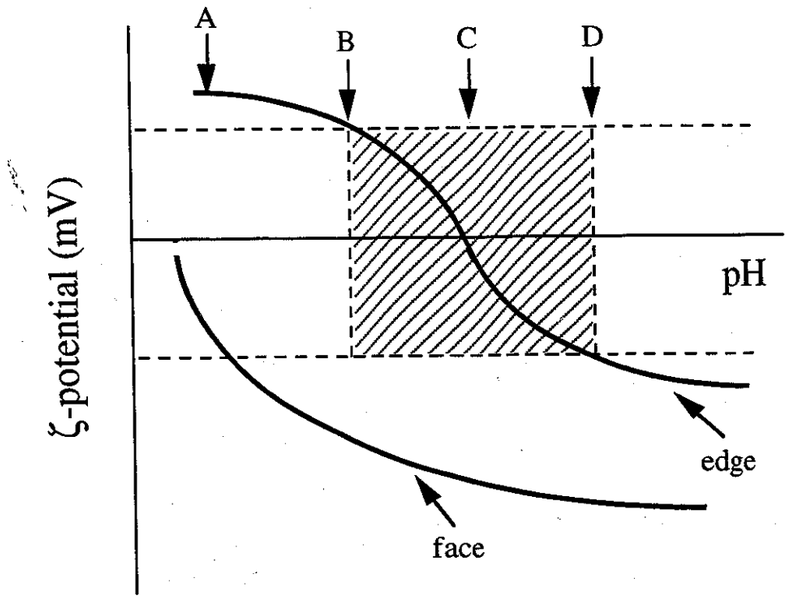

Figure 10 Theoretical interaction properties of the positive edge and negative face of the kaolinite particle as a function of pH. Designations explained in text.

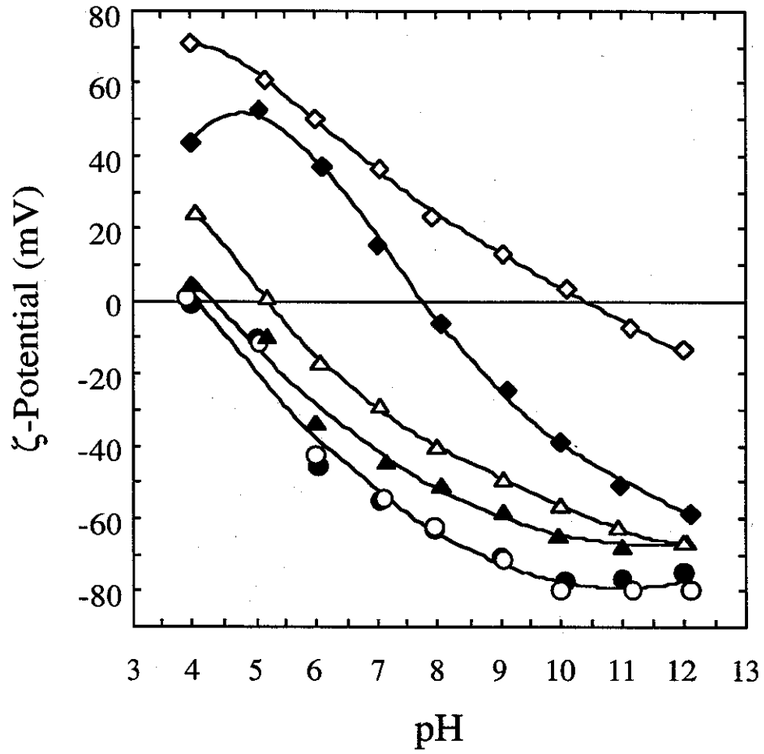

Figure 11 The ζ-potential as a function of both $AlCl_3$ concentration and pH for a 2.0 v/v % Weipa kaolinite / 10^{-3} mol dm^{-3} NaCl model system. ● = 0 dry weight based percent (dwb%) solids added $AlCl_3$; ○ = $2.5x10^{-3}$ dwb% $AlCl_3$; ▲ = $2.5x10^{-2}$ dwb% $AlCl_3$; △ = 0.25 dwb% $AlCl_3$; ◆ = 2.5 dwb% $AlCl_3$; ◇ = 25 dwb% $AlCl_3$.

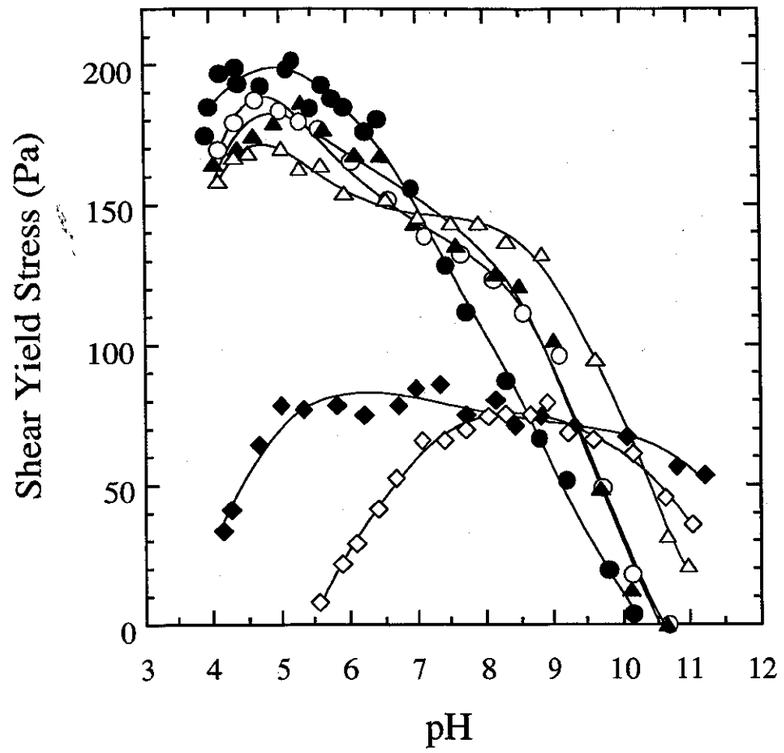

Figure 12 The shear yield stress as a function of both $AlCl_3$ concentration and pH for a 13.8 v/v% Weipa kaolinite / 10^{-3} mol dm^{-3} NaCl model system. ● = 0 dwb% $AlCl_3$; ○ = $2.5x10^{-3}$ dwb% $AlCl_3$; ▲ = $2.5x10^{-2}$ dwb% $AlCl_3$; △ = 0.25 dwb% $AlCl_3$; ◆ = 2.5 dwb% $AlCl_3$; ◇ = 25 dwb% $AlCl_3$.

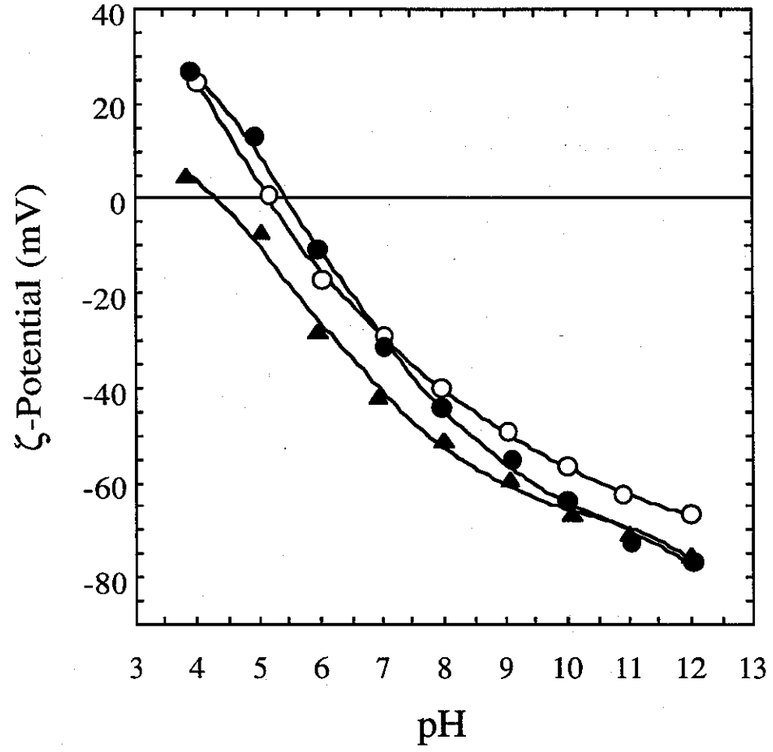

Figure 13 The ζ-potential as a function of both ($Al^{3+}{}_nX^{n-}{}_3$) concentration and pH for the 2.0 v/v% Weipa kaolinite / 10^{-3} mol dm^{-3} NaCl model system where ●: X = NO_3, n = 1; ○: X = Cl, n = 1; ▲: X = SO_4, n = 2.

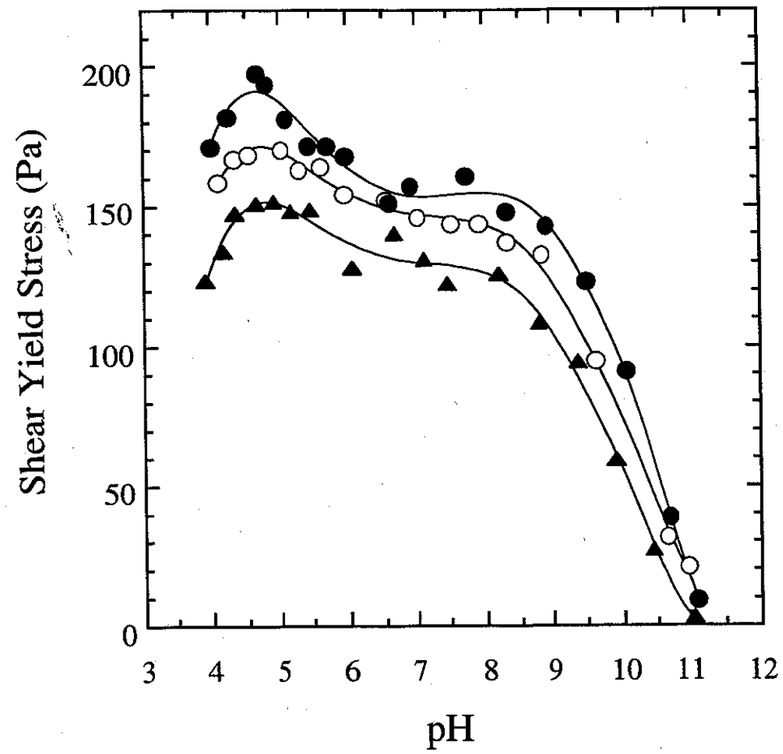

Figure 14 The shear yield stress as a function of both ($Al^{3+}_nX^{n-}_3$) concentration and pH for a 13.8 v/v % Weipa kaolinite / 10^{-3} mol dm^{-3} NaCl model system where ●: X = NO_3, n = 1; ○: X = Cl, n = 1; ▲: X = SO_4, n = 2.

Model Sludge Systems - Addition of Organic Components

Figure 15 shows the ζ-potential at pH 5.5 of a model raw water sludge consisting of silica and humics as a function of aluminium chloride concentration. The ζ-potential is seen to begin at a negative value but climb rapidly, passing through the pzc at *ca.* 0.6 dwb% $AlCl_3$. Beyond the pzc, the zeta potential continues to climb, reaching a ζ-potential of *ca.* 100 mV at an $AlCl_3$ concentration of 25 dwb%. The latter concentration is consistent with that used in the sweep flocculation process. On electrokinetic grounds, it may be expected that a low solids waste sludge would result relative to the case at the pzc, due to the large electrostatic repulsions in the system.

Table 1 Physical properties of a model silica/humic acid sludge and its supernatant after conditioning with various $AlCl_3$ concentrations.

[$AlCl_3$] (dwb%)	Sludge Solids (w/w %)	Supernatant Colour (Pt - Co Units)	Supernatant Turbidity (NTU)
0.6	14.3	30	15
1.3	13.9	15	9
25	6.6	5	17

Table 1 shows the silica/humic acid sludge volume fraction and supernatant colour and turbidity as a function of $AlCl_3$ concentration. The sludge shows a maximum weight fraction solids of 14.3 w/w % at 0.6 dwb% $AlCl_3$, which more than halves to 6.6 w/w % at 25 dwb% $AlCl_3$. Quite clearly, addition of excess quantities of aluminium produces a voluminous floc structure that resists consolidation, despite the high positive value of the zeta potential.

The supernatant turbidity remains constant within experimental error as a function of $AlCl_3$ concentration. However, the apparent colour shows a strong dependence upon the amount of aluminium present, with a large concentration being required to reduce the colour to an acceptable level. The humic acid is responsible for the residual colour observed. A large floc surface area is then required to adsorb these humics and reduce colour. The data is consistent with the postulate that in order to reduce alum concentrations to the level required to produce a

high solids sludge, development of an alternate method to sweep flocculation is necessary in order to remove persistent soluble organic components. This topic deserves further investigation. It is noteworthy that similar trends to those in Figure 15 and Table 1 are observed for the alternate use of ferric chloride as a flocculant. These data are shown in Appendix 1.

The ζ-potential of a real waste sludge as a function of pH is given in Figure 16. The sludge was obtained from sedimentation basin number one at Mount Crosby Westbank Water Treatment Plant. Although the quantity of alum contained in this sample is actually greater than the maximum concentration studied in Figure 15 (≈ 30 dwb %), the comparable ζ-potential (at pH 5.5) is both lower in magnitude and slightly negative. The probable explanation is the presence of a large quantity of particulate organics in the real sludge sample, which, due to the negative surface charge, would be anticipated to lower the average ζ-potential. It is also worth noting that the potential profile obtained bears little resemblance to that of the kaolinite/$AlCl_3$ system (Figure 11).

The data again emphasises the magnitude of the organic influence upon the sludge surface properties. Clearly, the humics suppress the effect of the alum by adsorbing to the flocs, creating a less positive surface. Despite the obvious differences between our model and real systems, the electrokinetic data on the model systems allows us to conclude that the real sludge is behaving as a humic rich alumina with very little influence of the underlying surface. The natural organic adsorbents are either of higher residual charge and/or substantially less soluble than the Aldrich humic acid utilised in this study.

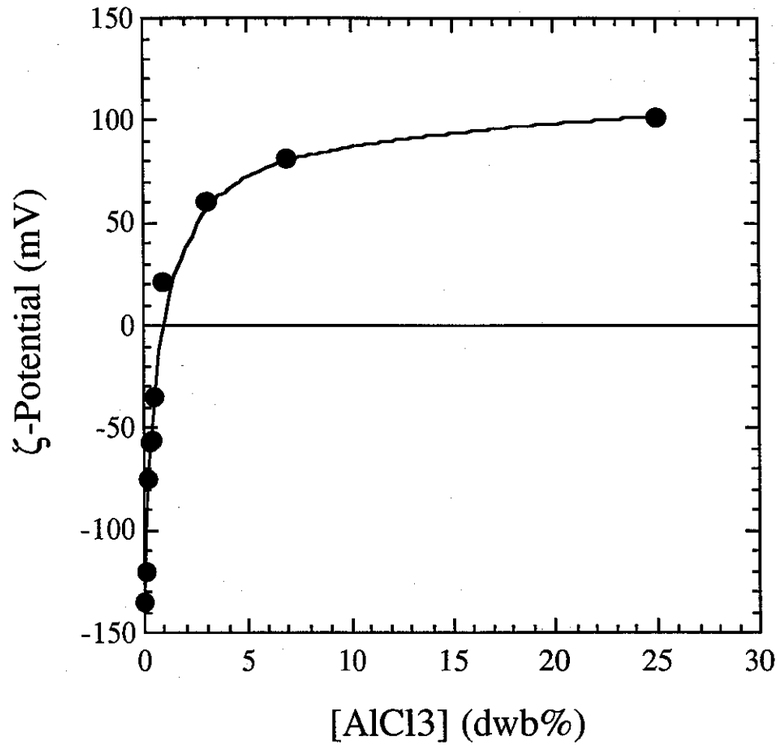

Figure 15 The ζ-potential as a function of $AlCl_3$ concentration at pH 5.5 for a 2.0 v/v % silica/humic acids model sludge.

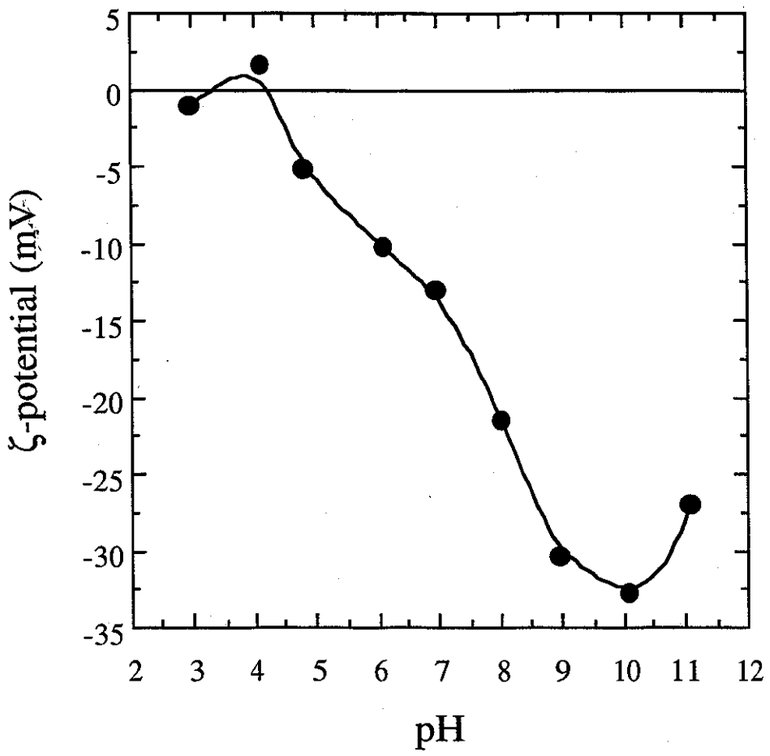

Figure 16 The ζ-potential as a function of pH for a potable water alum sludge system (ex. Mount Crosby Westbank Water Treatment Plant).

POLYELECTROLYTE FLOCCULATION PROCESSES

Treatment and subsequent dewatering of the raw sludge obtained from alum flocculation processes commonly involves addition of organic polyelectrolytes in order to improve dewatering properties. This is the case at the Mount Crosby Westbank Water Treatment Plant, as shown schematically in Figure 16. Raw sludge from the flocculation, DAF and filter backwashing processes is initially mixed in a holding tank. It is then pumped into a gravity thickener, receiving a polyelectrolyte dose of *ca.* 0.2 - 0.3 dwb % (2-3 kg/tonne of dry solids) as it enters the thickener feed well. After several hours light compression in the thickener, the sludge is discharged at a typical solids concentration of 2 - 3.5 w/w %. This is generally thickened to *ca.* 15 - 20 w/w% solids by high speed centrifugation after further polyelectrolyte addition and disposed of as landfill. Occasionally the 2 - 3.5 w/w % solids sludge is instead pumped to drying lagoons where it can take up to nine months to reach an acceptable solids level.

A number of factors are considered important to the use of organic conditioning agents, not the least being selection of the type and dose rate of polyelectrolyte used. The shear intensity and time of mixing of the polyelectrolyte with the raw sludge is also critical [23]. The optimum choice of flocculant, dose, and mixing time and intensity has traditionally been regarded as that which provides the most rapid initial rate of dewatering [20]. By contrast, relatively little work to date has focussed upon the effect of the polyelectrolyte addition on the sludge compressibility properties.

The influence of the type of polyelectrolyte and the polyelectrolyte dose rate on the compression and dewatering properties of the conditioned sludge is now examined. The mixing times and intensities have been optimised with regard to dewatering, and then kept constant between samples. The influence of shear should therefore have little bearing upon the results.

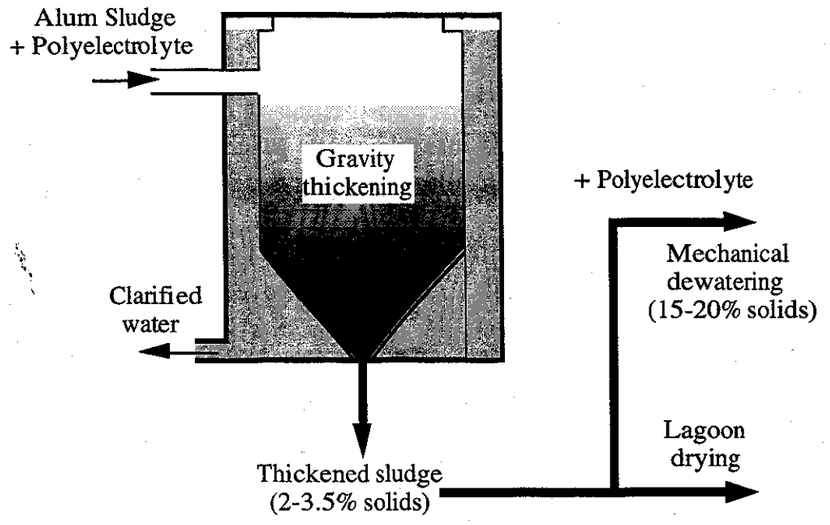

Figure 17 The use of organic polyelectrolytes in the alum sludge thickening process at the Mount Crosby Westbank Water Treatment Plant.

Experimental Section

Raw alum sludge samples were obtained from sedimentation basin number one at Mount Crosby Westbank Water Treatment Plant. The sludge was typically between 1.2 and 1.5 w/w % solids.

A range of high molecular weight polyelectrolytes (LT Magnaflocs) were obtained from Allied Colloids Ltd. These were of varying MW and anionic charge density, as shown in Table 2. Anionic polyelectrolytes were used in preference to cationic, due to the requirement of binding to the positively charged alum floc structure.

Table 2 The relative molecular weights and anionic charge densities of the LT range of organic polyelectrolytes used in this study.

Charge Density	High MW	Very High MW
high	-	LT-30
medium	LT-26	LT-27
low	LT-25	LT-25S
zero	LT-20	-

Organic polyelectrolyte solutions were prepared as suggested by the manufacturer. The dry polyelectrolyte was initially wet with a small volume of analytical grade ethanol. Water was then added, and the sample sheared for *ca.* 30 minutes before use. Mixing of the alum sludges and organic polyelectrolytes was again performed according to specifications given by the manufacturer. The combined mixtures were stirred vigorously at *ca.* 120 rpm for 30 seconds, followed by gentle stirring at *ca.* 30 rpm for a further 450 seconds. They were then allowed to stand and settle undisturbed.

Electrokinetic characterisation of the sludge - polyelectrolyte surface interactions could not be performed in this case, due to the size of the flocs formed being in excess of the maximum

particle size capacity of the Acoustosizer. Rheological measurements were made using techniques previously outlined. The initial rate of dewatering was measured utilising the Capillary Suction Time (CST) technique of Baskerville and Gale [24]. This instrument uses an automatic timing device to follow the initial filtration rate out of the sludge system. Filtration is achieved by the suction applied to the sludge by the capillary action of a standard absorbent chromatography filter paper.

The Polyelectrolyte Flocculated Alum Sludge System

The CST as a function of both organic polyelectrolyte type and concentration is shown in Figures 18 (a) and (b). All samples were prepared as described previously, then compressed to 6 w/w % (2.3 v/v %) for CST analysis. This latter process was undertaken in order to increase the magnitude of the measured CST value as the errors inherent in the technique are significant at low ϕ. Although reproducibility of results remained a problem, with variation in measured CST's of up to 50 percent not uncommon, the thickening of the sludge samples allowed the dose dependence trends of the various polyelectrolytes to be more easily distinguished. As shown in Figures 18 (a) and (b), the minimum in the measured CST value generally occurred with polyelectrolyte doses of between 0.2 and 0.6 dwb % (2-6 kg/tonne of dry solids). Whilst the individual polyelectrolyte systems displayed quite different dose dependence, particularly at low polyelectrolyte concentrations, the data does not display any obvious charge density or molecular weight related trends.

Figures 19 (a), (b) and (c) shows the compressive yield stress behaviour of the various polyelectrolyte flocculated sludge systems for three different polyelectrolyte concentrations. The results show almost identical compression behaviour for the range of polyelectrolytes investigated, despite the significant charge density and molecular weight differences illustrated in Table 2. The implication of these results is that the dominant mechanism of action of the polyelectrolytes in the alum flocculated sludge system is most probably in inter-particle bridging. The mechanism of surface charge neutralisation invoked from adsorption of these molecules, whilst obviously present, appears insignificant to the sludge compressional properties.

The results displayed in Figures 18 (a) and (b) additionally show the flocculated sludge compression properties to be largely dose independent over the polyelectrolyte concentrations studied. On this basis, the selection of an appropriate organic polyelectrolyte type and dose can be based purely upon the optimum dewatering and handleability (viscosity) properties generated by the chosen polyelectrolyte.

The data in Figures 18 and 19 represent a unique study of the influence of high molecular weight polyelectrolytes on the compressibility of alum rich potable water sludges. The results indicate that the compressibility of these systems (ie. the ability to dewater effectively) is totally dominated by the presence of alum.

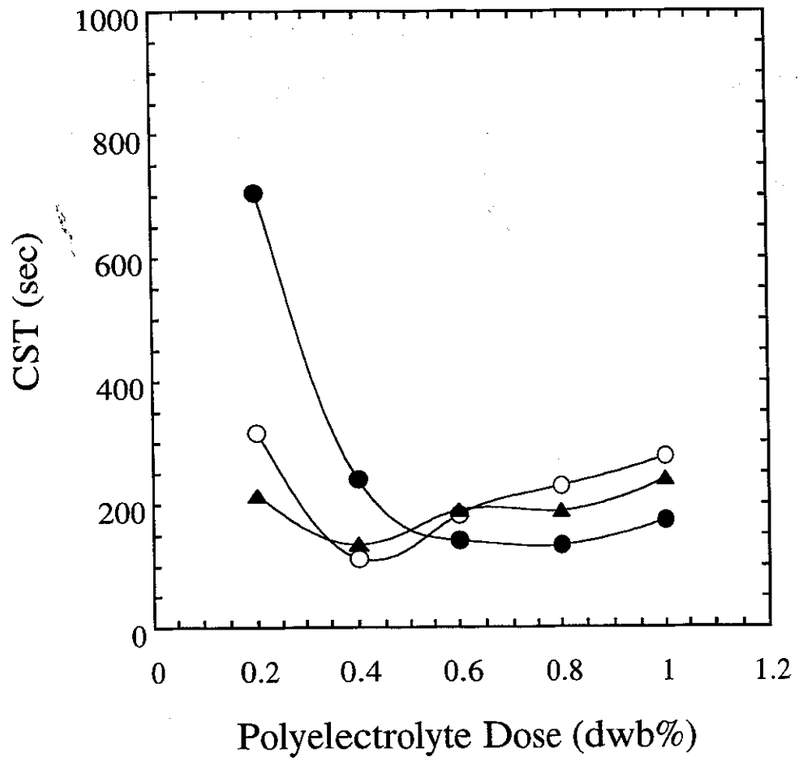

Figure 18(a) The Capillary Suction Time (CST) as a function of both organic polyelectrolyte type and concentration for the raw alum flocculated sludge system. ● = LT-20; O = LT-25; ▲ = LT-25S.

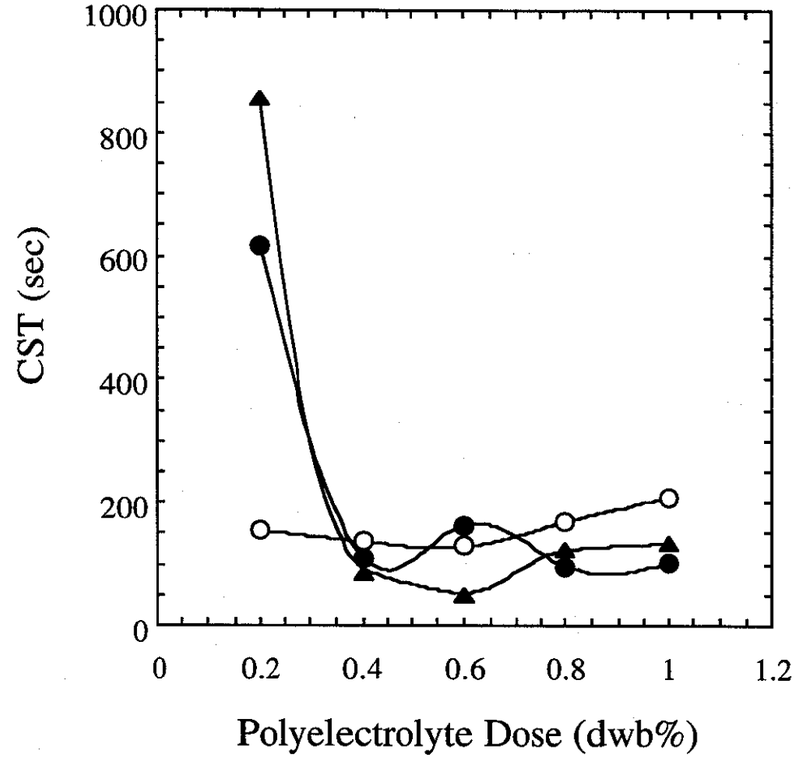

Figure 18(b) The Capillary Suction Time (CST) as a function of both organic polyelectrolyte type and concentration for the raw alum flocculated sludge system. ● = LT-26; O = LT-27; ▲ = LT-30.

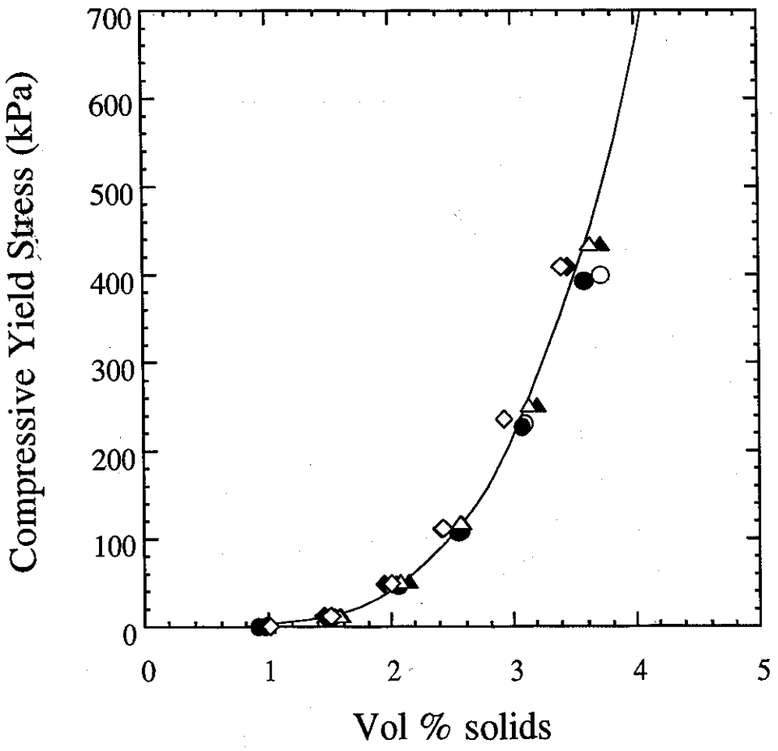

Figure 19(a) The compressive yield stress as a function of both organic polyelectrolyte type and alum sludge solids volume fraction. In all cases, the polyelectrolyte concentration is 0.2 dwb%. ● = LT-20; ○ = LT-25; ▲ = LT-25S; △ = LT-26; ◆ = LT-27; ◇ = LT-30. The line plot represents the compressive properties of the raw sludge in the absence of polyelectrolyte additives.

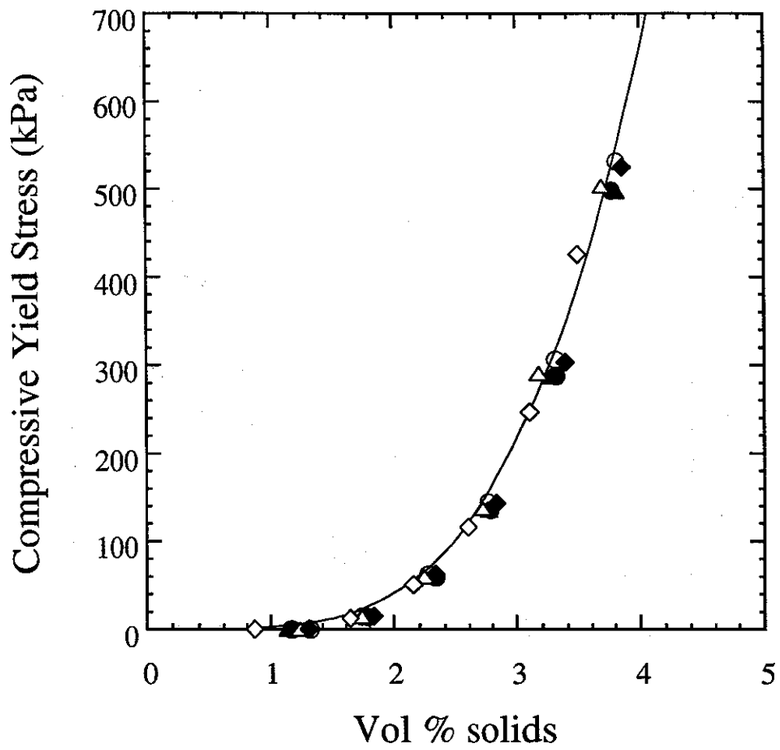

Figure 19(b) The compressive yield stress as a function of both organic polyelectrolyte type and alum sludge solids volume fraction. In all cases, the polyelectrolyte concentration is 0.4 dwb%. ● = LT-20; ○ = LT-25; ▲ = LT-25S; △ = LT-26; ◆ = LT-27; ◇ = LT-30. The line plot represents the compressive properties of the raw sludge in the absence of polyelectrolyte additives.

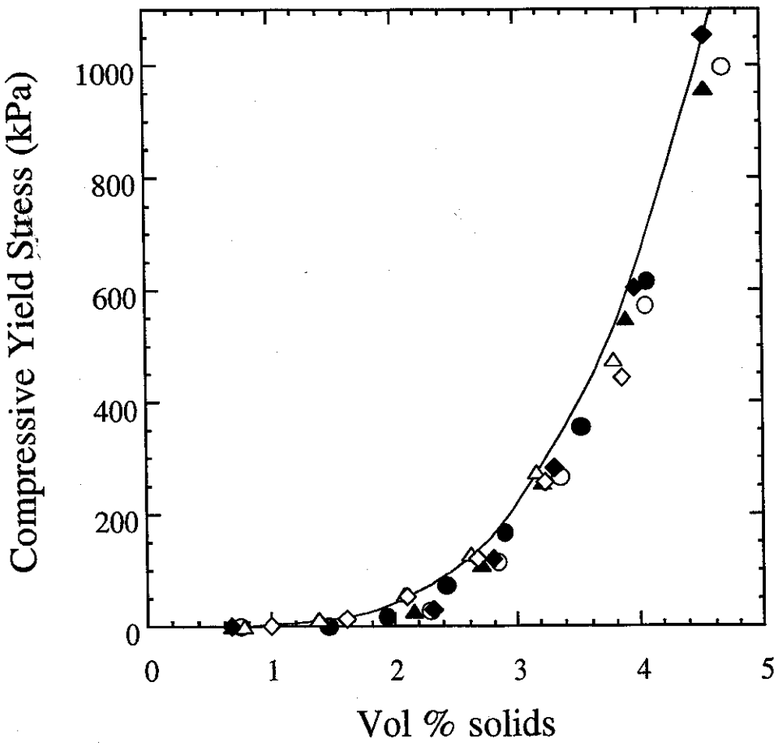

Figure 19(c) The compressive yield stress as a function of both organic polyelectrolyte type and alum sludge solids volume fraction. In all cases, the polyelectrolyte concentration is 0.6 dwb%. ● = LT-20; ○ = LT-25; ▲ = LT-25S; △ = LT-26; ◆ = LT-27; ◇ = LT-30. The line plot represents the compressive properties of the raw sludge in the absence of polyelectrolyte additives.

APPLICATION OF LOW MOLECULAR WEIGHT HYDROPHILIC MOLECULES TO ALUM SLUDGE THICKENING

The possible use of low MW hydrophilic molecules to control the surface interaction and rheological properties of particulate suspensions is a relatively recent innovation [4, 5]. The mechanism of action involves surface adsorption of a species of opposite charge to that of the surface. Electrokinetically, this has the effect of modifying the surface charge properties, and so the position of the pzc, as a function of the pH of the suspension. Rheologically, it is postulated that the molecule acts as a steric barrier to close particle approach, so lowering the shear and compressive yield stresses.

An appropriate method of utilising the steric behaviour of low MW additives would be to flocculate a suspension, either by adjusting the pH to the pzc or using chemical flocculants, and then use the low MW additives to partially sterically destabilise the resulting floc structure [1]. A more compressible flocculated sludge should then result, leading to a higher solids final waste product.

Table 3 shows the limiting maximum shear yield stress, $\tau_y(\phi)_{max}$, and the effective thickness of the adsorbate layer on the colloidal particle surface, δ, for the adsorption of a number of anionic low MW hydrophilic molecules on zirconia, ZrO_2 [5]. As was demonstrated, a large δ corresponds to a greater extent of maximum yield stress reduction.

The use of an anionic molecular steric barrier is appropriate for use with the positive surface charge carried by the alum flocculant. Of the molecules shown in Table 3, citrate and malate anions gave rise to the largest steric barrier thicknesses. These were chosen for use in this study.

Table 3 Variation of the maximum yield stress of a 57 w/w% (9.5 v/v%) ZrO_2 suspension with the surface steric barrier thickness generated by a number of low MW anionic molecules [5].

Low MW anion	$\tau_y(\phi)_{max}$ (Pa)	δ (Å)
None	440	-
Sulphate	269	1.26
Phosphate	205	1.94
Pyrophosphate	200	2.02
1,2,3-BTC	145	3.28
Lactate	135	3.61
Malate	134	3.64
Citrate	99	5.26

Experimental Section

AKP-30 alumina in the presence of 10^{-3} mol dm^{-3} NaCl was used as a model aluminium-based system. Citrate and malate were obtained in their acid forms as analytical grade citric and laboratory grade maleic acids. Adjustment of system pH was performed with analytical grade HCl and NaOH.

Raw alum sludge samples were obtained from sedimentation basin number one at Mount Crosby Westbank Water Treatment Plant. To allow citrate and malate penetration of the alum sludge structure, it was dispersed slightly with pH adjustment to a pH of *ca.* 9.0. Destabilisation of the floc structure was therefore attempted with the two-fold mechanism of double layer compression and steric hindrance. Flocculation was performed with the non-ionic organic polyelectrolyte LT-20 as previously described. A suite of electrokinetic and rheological measurements were made on each sample.

Results and Discussion

Citrate Modification of the Model Alumina Surface

The dependence of the AKP-30 alumina ζ-potential and shear yield stress values upon both pH and citric acid concentration are shown in Figures 20 and 21 respectively. The electroacoustic results demonstrate a marked shift in the position of the pzc as the citric acid concentration is increased. Zeta potentials are observed to drop as citric acid dosage is increased, presumably due to the adsorption of the citrate ion on the alumina surface. Values of $\tau_y(\phi)$ decrease substantially with addition of low citric acid concentrations, as is anticipated for the addition of a surface adsorbed steric barrier to modulate close inter-particle approach. With more substantial citric acid concentrations, however, alumina shear yield stresses are observed to taper off, and then rise with concentrations beyond *ca.* 0.2 dwb% additive. This latter behaviour was both unexpected and intriguing.

A possible explanation is the swelling of alumina surfaces due to partial gelation when approaching dissolution pH conditions. An increase in colloidal surface area would result, and, if large enough, would result in an increase in the yield stress. A second possibility is a mechanism of citrate solution agglomeration, and corresponding surface depletion, at the higher citrate concentrations. Whatever the mechanism at low pH, at pH's of interest to sludge treatment in the water industry, the citrate ion is a very effective dispersant for model alumina particles. An interesting aside is the similarity of the form of the high citrate dose curves in Figure 20 and the real alum based sludge shown in Figure 16.

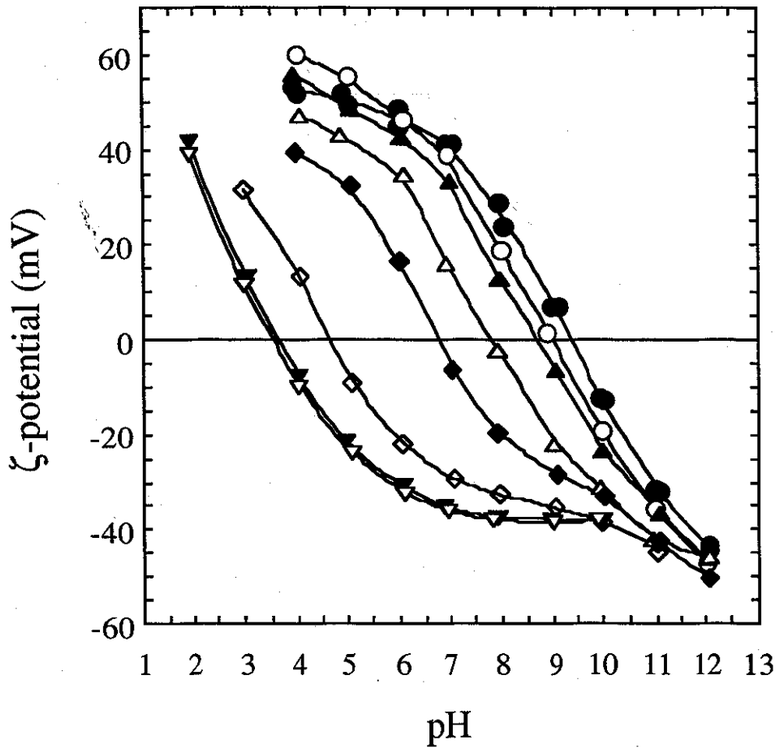

Figure 20 The ζ-potential as a function of both citric acid concentration and pH for the 2.0 v/v% AKP-30 alumina / 10^{-3} mol dm^{-3} NaCl model system. ● = 0 dwb% citric acid; ○ = 0.01 dwb% citric acid; ▲ = 0.02 dwb% citric acid; △ = 0.06 dwb% citric acid; ◆ = 0.10 dwb% citric acid; ◇ = 0.20 dwb% citric acid; ▼ = 0.50 dwb% citric acid; ▽ = 0.80 dwb% citric acid.

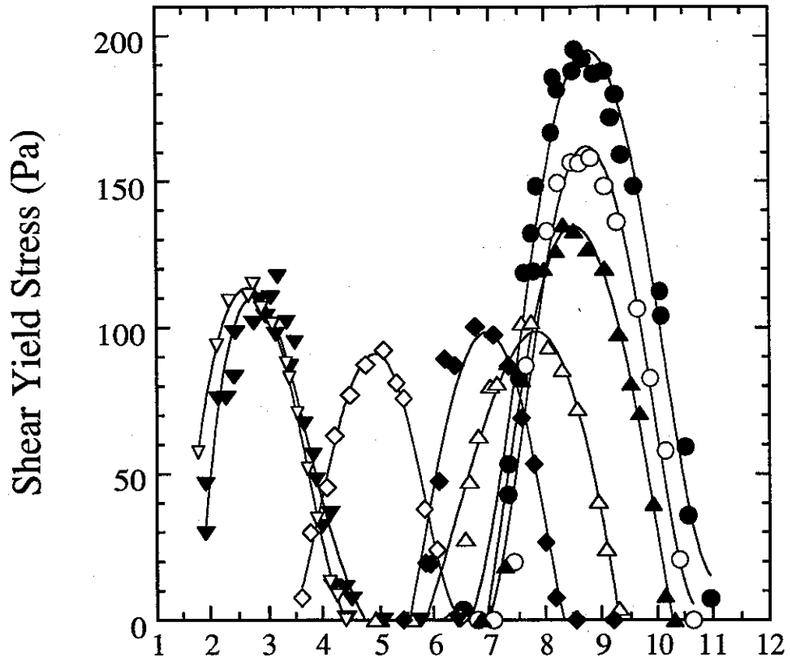

Figure 21 The shear yield stress as a function of both citric acid concentration and pH for the 2.0 v/v% AKP-30 alumina / 10^{-3} mol dm^{-3} NaCl model system. ● = 0 dwb% citric acid; ○ = 0.01 dwb% citric acid; ▲ = 0.02 dwb% citric acid; △ = 0.06 dwb% citric acid; ◆ = 0.10 dwb% citric acid; ◇ = 0.20 dwb% citric acid; ▼ = 0.50 dwb% citric acid; ▽ = 0.80 dwb% citric acid.

Citrate and Malate Modification of the Alum Sludge Surface

Figure 22 shows the raw alum sludge ζ-potential as a function of both pH and citric and maleic acid concentrations. The addition of citric and maleic acids has no significant effect upon the sludge surface charge.

The dependence of the alum sludge compressive yield stress upon both citric and maleic acid concentrations are shown respectively for three LT-20 concentrations in Figures 23 and 24. Shifting the system from its natural pH to pH 9.0 produced a slight improvement in the compressive yield stress. However, the addition of citric and maleic acids failed to further enhance the compression properties of the system. The results also demonstrate the independence of the compression properties from the organic polyelectrolyte concentration, as shown in Figure 19.

The failure of the citrate and malate anions to favourably modify the alum sludge compression properties is disappointing. At high humic loadings (as appears the case in this study), it may be that humic acid complexation of the alum surface is so extensive as to preclude the adsorption of more soluble dispersants such as citrate and malate. The data serves to demonstrate that, as with the addition of polyelectrolyte, the alum floc structure is difficult to chemically rearrange and the presence of humics makes this even more difficult. The result is a direct consequence of the practice of using high alum doses to not only remove particulates but also to remove colour. The large amount of additional alum required for the colour removal dominates the compressibility of the sludge. While this practice persists, the chemical modification of the compressibility of alum based sludges will remain extremely difficult.

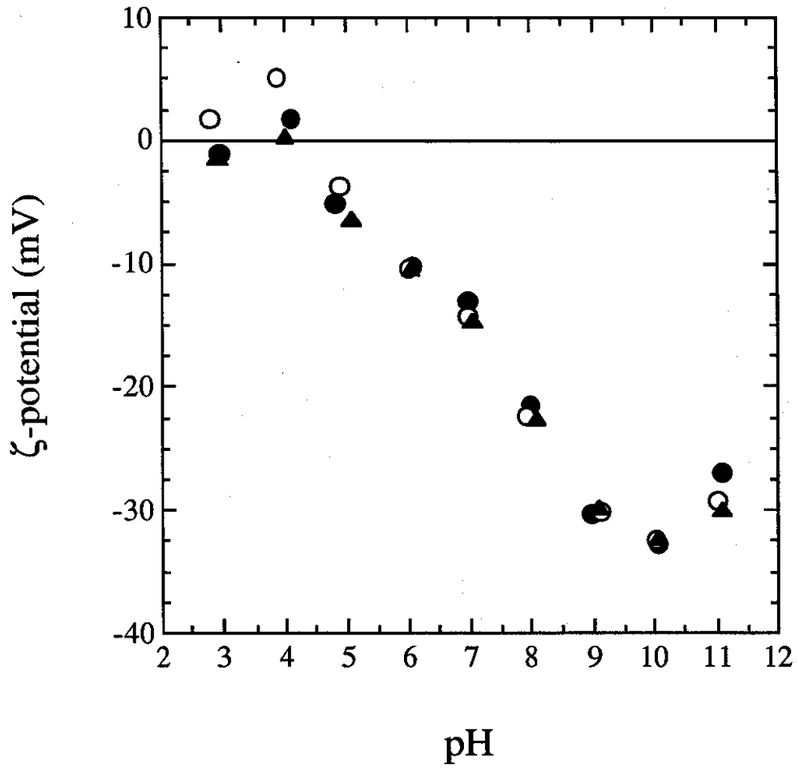

Figure 22 The ζ-potential as a function of both low MW steric additive type and pH for the raw alum flocculated sludge system. ● = 0 dwb% additive; ○ = 0.20 dwb% citric acid; ▲ = 0.20 dwb% maleic acid.

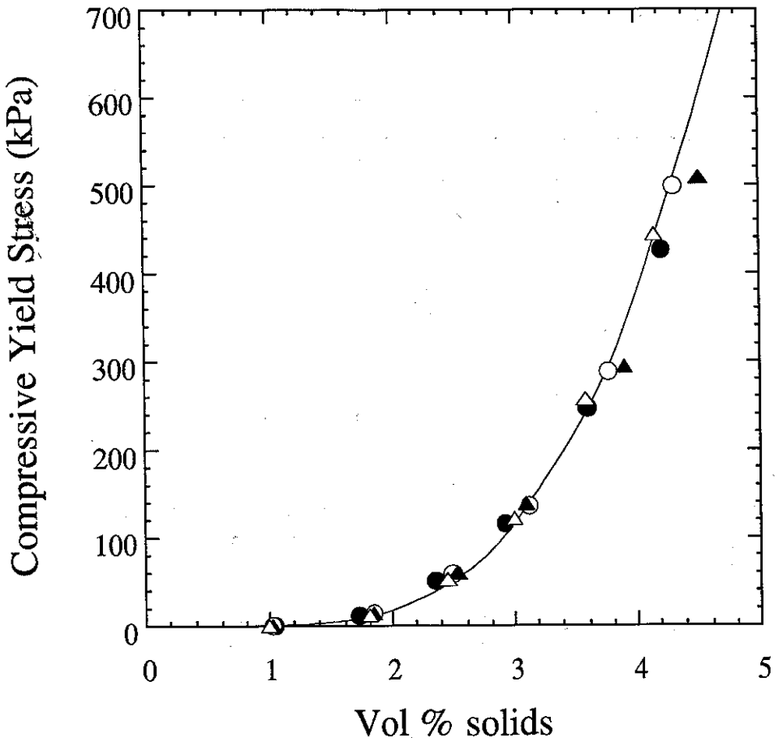

Figure 23(a) The compressive yield stress as a function of both citric acid concentration and volume fraction for the 0.2 dwb% LT-20 / alum flocculated sludge system at pH 9. ● = 0.05 dwb% citric acid; ○ = 0.10 dwb% citric acid; ▲ = 0.15 dwb% citric acid; △ = 0.20 dwb% citric acid. The line plot represents the compressive properties of the 0.2 dwb% LT-20 / alum flocculated sludge system at pH 9 in the absence of citric acid.

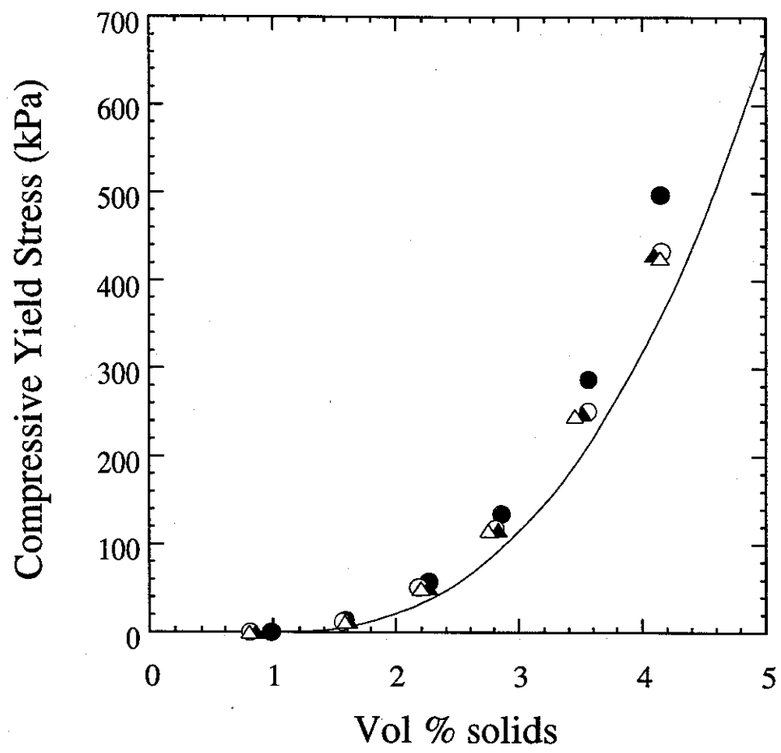

Figure 23(b) The compressive yield stress as a function of both citric acid concentration and volume fraction for the 0.4 dwb% LT-20 / alum flocculated sludge system at pH 9. ● = 0.05 dwb% citric acid; ○ = 0.10 dwb% citric acid; ▲ = 0.15 dwb% citric acid; △ = 0.20 dwb% citric acid. The line plot represents the compressive properties of the 0.4 dwb% LT-20 / alum flocculated sludge system at pH 9 in the absence of citric acid.

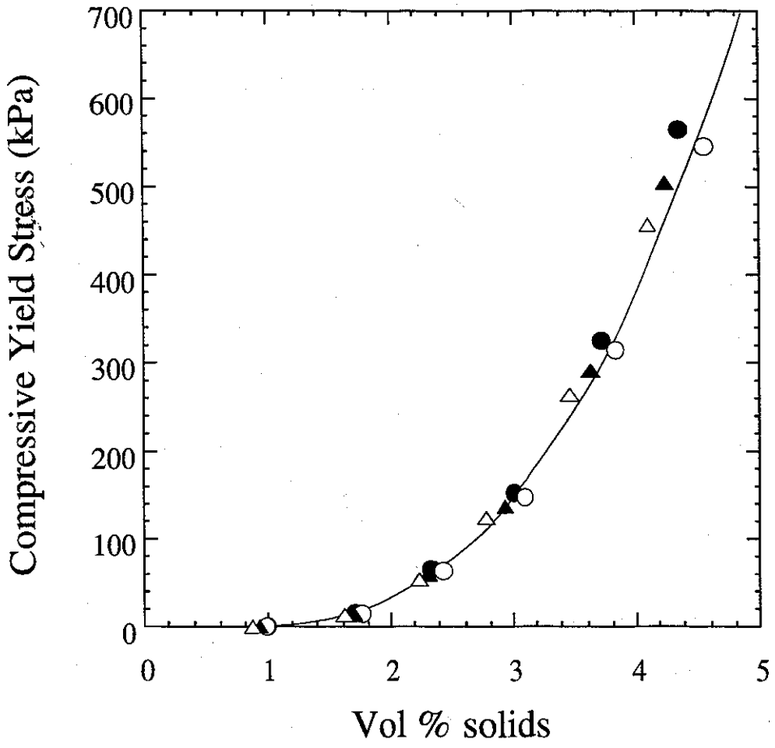

Figure 23(c) The compressive yield stress as a function of both citric acid concentration and volume fraction for the 0.6 dwb% LT-20 / alum flocculated sludge system at pH 9. ● = 0.05 dwb% citric acid; ○ = 0.10 dwb% citric acid; ▲ = 0.15 dwb% citric acid; △ = 0.20 dwb% citric acid. The line plot represents the compressive properties of the 0.6 dwb% LT-20 / alum flocculated sludge system at pH 9 in the absence of citric acid.

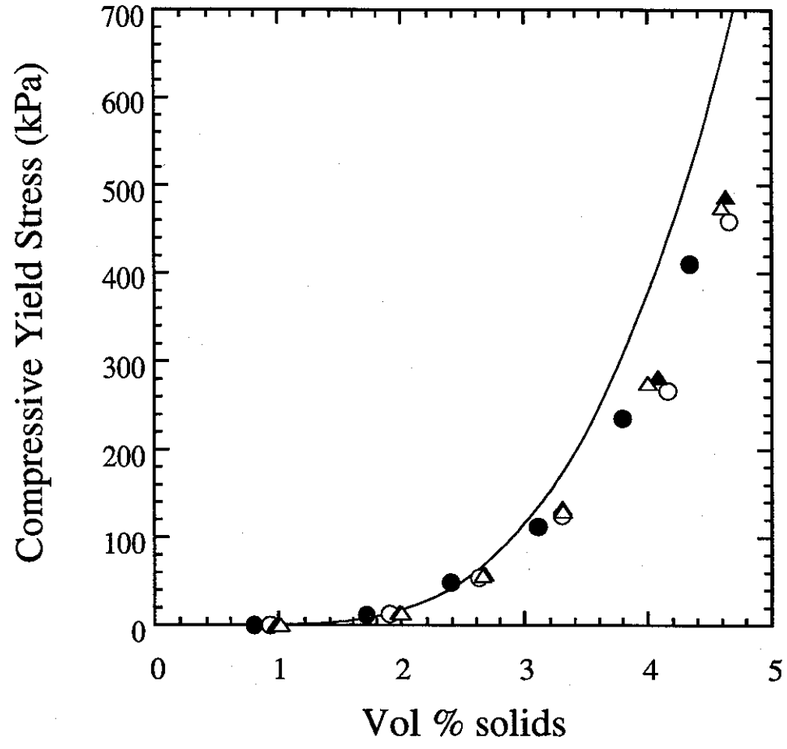

Figure 24(a) The compressive yield stress as a function of both maleic acid concentration and volume fraction for the 0.2 dwb% LT-20 / alum flocculated sludge system at pH 9. ● = 0.05 dwb% maleic acid; ○ = 0.10 dwb% maleic acid; ▲ = 0.15 dwb% maleic acid; △ = 0.20 dwb% maleic acid. The line plot represents the compressive properties of the 0.2 dwb% LT-20/alum flocculated sludge system at pH 9 in the absence of maleic acid.

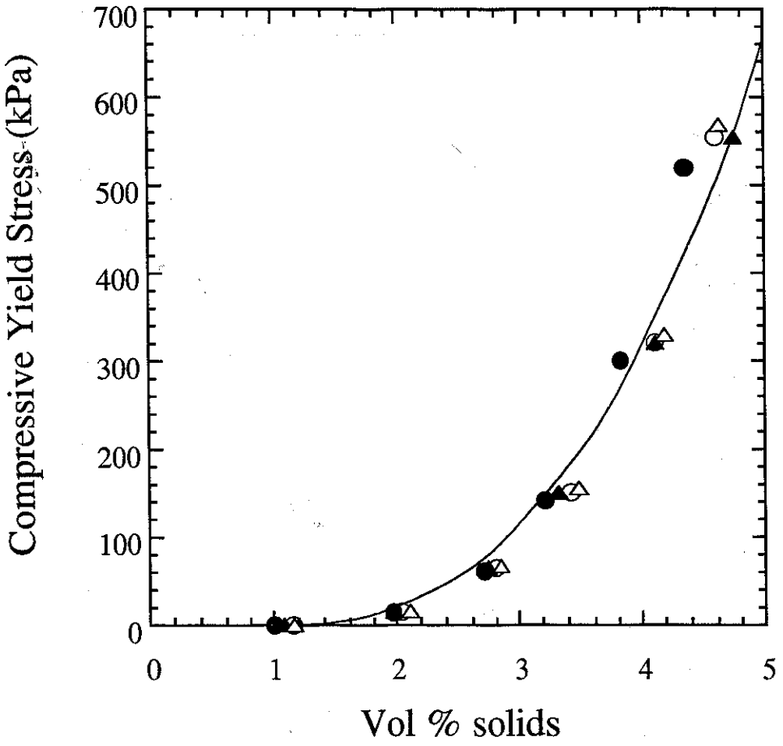

Figure 24(b) The compressive yield stress as a function of both maleic acid concentration and volume fraction for the 0.4 dwb% LT-20 / alum flocculated sludge system at pH 9. ● = 0.05 dwb% maleic acid; ○ = 0.10 dwb% maleic acid; ▲ = 0.15 dwb% maleic acid; △ = 0.20 dwb% maleic acid. The line plot represents the compressive properties of the 0.4 dwb% LT-20 / alum flocculated sludge system at pH 9 in the absence of maleic acid.

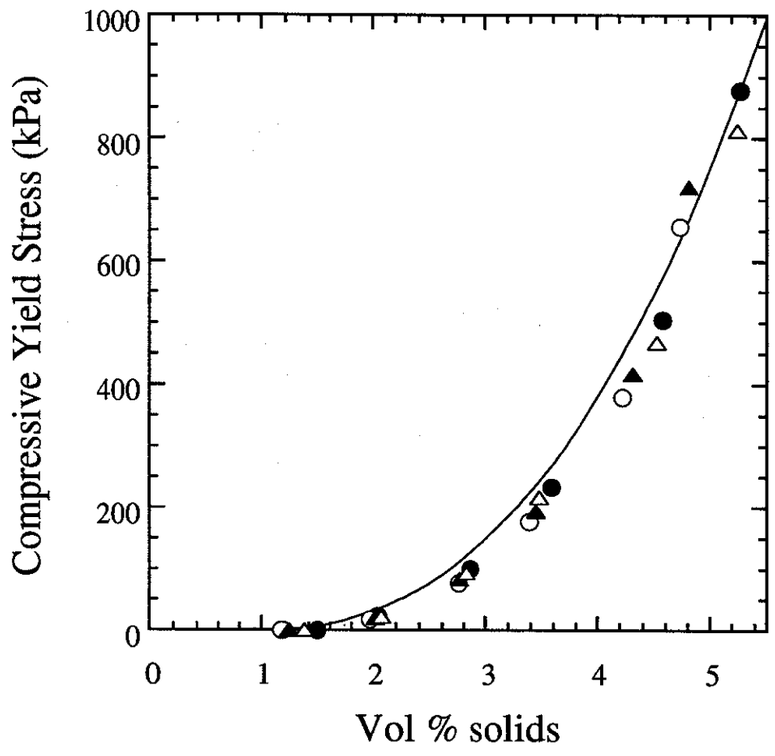

Figure 24(c) The compressive yield stress as a function of both maleic acid concentration and volume fraction for the 0.6 dwb% LT-20 / alum flocculated sludge system at pH 9. ● = 0.05 dwb% maleic acid; ○ = 0.10 dwb% maleic acid; ▲ = 0.15 dwb% maleic acid; △ = 0.20 dwb% maleic acid. The line plot represents the compressive properties of the 0.6 dwb% LT-20/alum flocculated sludge system at pH 9 in the absence of maleic acid.

High Speed Centrifuge Tests

Despite the lack of success in the modification of the chemical structure of the alum rich sludge, a number of tests were performed on the high speed centrifuge to examine the role of additives, time and shear in the dewatering process at full scale. Examination of the compressibility data from Figures 19, 23 and 24 indicates that a maximum expected volume fraction solids under equilibrium centrifugation conditions should be of order 5 volume % (12-13 w/w %) solids. On-site results show this to be a slight under-estimate of the results obtained using the high speed plant centrifugation, which typically produces sludges of 16-17 w/w % solids. Operationally, the feed slurry to the centrifuge needs to be heavily flocculated to withstand the shear forces in the centrifuge and maintain filtrate clarity. These same shear forces appear none the less to be beneficial to the dewatering process, despite the fact that the addition of polymer is almost certainly limits the total achievable solids.

Two aspects of the process were examined;

- Could flocculant dose be reduced or could dosing be more effective given that the main role of the flocculant addition other than to increase permeability was to give the floc structure enough rigidity to withstand shear in centrifugation? Shear in pumping is almost certainly detrimental to polymer effectiveness if the floc structure is already destroyed.

- Does dispersion of the flocculated feed slurry to the centrifuge with low MW dispersants such as citrate increase the solids output? This test was completed despite the poor laboratory result because penetration of the citrate in the floc structure was considered more viable at full scale under high shear conditions.

To examine the first hypothesis, the entire floc dose (*ca.* 0.6 dwb %) was added prior to thickening. Current practice is to dose prior to the thickener and again immediately prior to the centrifuge (after the centrifuge feed pump). The result was formation of a significantly more robust floc structure which is better able to withstand the vigorous shear forces created during pumping of the sludge between the gravity thickener and the centrifuge. The high shear nature

of the pumping process is undesirable but is unavoidable in some instances. The test produced a cake of *ca.* 7 volume per cent or 18-19 w/w % solids sludge which is significantly above the range of solids predicted in Figure 24., A possible explanation for this result is the large shear force acting at the point at which the gravity thickened sludge comes into contact with the rapidly spinning sludge cake in the plant centrifuge. The mechanism and consequences of such a sudden shear force, although unclear, presumably relate to the weakness of the sludge in shear relative to compression.

Tests were also performed with the addition of a dispersant, namely citrate, to the sludge. The centrifuge produced an output comparable to the 18-19 w/w % solids described above but at a significantly lower viscosity. This was an encouraging result in that it shows the expected trend in terms of dispersion but reflects that the solids residence time in the centrifuge was insufficient. A consequence of dispersion is that the permeability and thus dewatering time will increase. With no easy way to adjust the residence time in the device, the full potential of the use of dispersants could not be established.

In summary, the initial examination of the role of shear forces in dewatering shows that benefit can be gained provided the shear forces are optimised to the strength of the particulate network. The result is that either polymer dose could be reduced or solids increased if more careful attention was paid to the level and application of shear in both pumping and the dewatering process. Dispersion of the sludge prior to polymer flocculation also appeared beneficial although current dewatering devices are poorly engineered to exploit this sludge attribute.

CONCLUSIONS and RECOMMENDATIONS

The results of the present study provide some new and important insights into the dewatering of alum rich potable water sludges. The main findings and recommendations are;

The sweep flocculation process, whilst necessary to remove colour from water, produces an alum rich sludge that has a low gel point and is difficult to compress. The addition of flocculants gives the floc structure some rigidity but only aids the rate of dewatering, not the extent of dewatering. The floc structure is thus totally dominated by the alum.

Recommendation: Development of an alternative method to the use of alum for the removal of colour would allow a significant reduction in alum use and improve the compressibility of sludges considerably.

The results of this study indicate that the level of use of high MW polyelectrolytes in sludge conditioning prior to centrifugal dewatering is optimised to produce enough floc rigidity to withstand the centrifugation process but the optimal rate of dewatering (based on permeability analysis) is achieved at a lower dose rate.

Recommendation: That the application of shear in the transfer of sludges (ie. in pumping) and in the centrifuge feed be minimized where possible to reduce flocculant dose requirements.

The role of humic materials in natural water systems and in sweep flocculation is to produce a sludge that has a net negative surface charge. This is vastly different to the model sludge situation where the same level of alum dosing produces a net positive surface charge on the sludge. The consequence of the presence of humics is that the floc structure is poorly receptive to low MW dispersants that may be of use in sludge dispersion and ultimately, higher solids sludge production.

Recommendation: Studies on model sludges should always include the role of humics of an appropriate type and concentration or preferably, work should concentrate where possible on actual Water Treatment Plant sludges.

The mechanical instability of alum flocs and the low relative density are the main restraints to producing high solids loading sludges. Techniques that do not provide shear in excess of the shear stress of the suspensions but simply let water drain from the suspension need to be examined in more detail. The implication of this finding is that even the rate of shear supplied by devices such as the rakes in clarifiers should be re-evaluated.

Recommendation: That static and low pressure dewatering devices be considered in preference to high pressure devices based on the incompressibility of the sludges.

The study shows that for alum rich sludges there is little or no dependence on the extent of dewatering of either chain length or charge type and density for high MW polyelectrolytes, provided they are used in excess of the minimum CST value. This is nearly always the case in practice.

Recommendation: Polymer use in dewatering of high alum content sludges should be optimised on polymer handling efficiency, the sludge permeability at a given dose and cost . This is based on the observation that there is little dependence of polymer type or charge on sludge compressibility.

The results achieved at a laboratory scale for the prediction of dewatering behaviour using a centrifugal technique were similar to that achieved at full scale, except where high shear processes were involved. The data indicates that the essential physics of the dewatering process are being well represented by the current compressibility models.

Recommendation: That compressibility tests be considered in conjunction with permeability (CST) tests wherever sludge dewatering was being evaluated. This is especially relevant if process alternatives to sweep coagulation using alum are being considered.

ACKNOWLEDGMENTS

The authors acknowledge the funding of this project by the Urban Water Research Association of Australia and infrastructure support from the Advanced Mineral Products Special Research Centre, a Special Research Centre of the Australian Research Council. In particular, the on-site help at Mount Crosby Westbank Water Treatment Plant near Brisbane supplied by Mr Rob Townsley, the plant operators and maintenance staff is gratefully acknowledged. The authors would also like to thank Allied Colloids for donating the range of polymers used in this study.

REFERENCES

1 TW Healy, DV Boger, LR White, PJ Scales and YK Leong (1994),*Thickening and clarification; How much do we really know about dewatering*, 6th AusIMM Extractive Metallurgy Conference, Brisbane, Australia, July 1994

2 R Buscall and LR White (1987), *The consolidation of concentrated suspensions*, J. Chem. Soc. Faraday Trans. I, 83: 873-891.

3 M Eberl, KA Landman and PJ Scales (1995), *Scale-up procedures and test methods in filtration: a test case on kaolin plant data*, Colloids and Surfaces A; Physicochemical and Engineering Aspects, 103: 1-10.

4 YK Leong, DV Boger, PJ Scales, TW Healy and R Buscall (1993), *Control of the rheology of concentrated aqueous colloidal systems by steric and hydrophobic forces*, J. Chem. Soc. Chem Communications, 7: 639-641.

5 YK Leong, DV Boger, PJ Scales, TW Healy and R Buscall (1993), *Rheological evidence of adsorbate mediated short range steric forces in concentrated dispersions*, *J. Chem. Soc. Faraday Trans*, 89: 2473-2478.

6 W Barron, BS Murray, PJ Scales, TW Healy, DR Dixon and M Pascoe (1994), *The streaming current detector: A comparison with conventional electrokinetic techniques*, Colloids and Surfaces A; Physicochemical and Engineering Aspects, 88: 129-140.

7 A Amirtharajah (1982), *Water treatment plant design*, RL Sanks (Editor), Ann Arbor, Michigan, USA, 131-147.

8 A Amirtharajah and MM Clark (1991), *Mixing in coagulation and flocculation*, AWWA Research Foundation, Denver, USA, 3-7.

9 RJ Hunter (1981), *Zeta Potential in Colloid Science*, London, UK, Academic Press.

10 PJ Debye (1933), *A method for the determination of the mass of electrolytic ions*, Journal of Chemical Physics, 1: 13.

11 R Zana and E Yeager (1982), *Ultrasonic vibration potentials*, in Modern Aspects of Electrochemistry, Volume 14, J.O.M. Bockris (Editor), Plenum Press, New York, USA.

12 T Oja, GL Petersen and DW Cannon (1985),*United States Patent No. 4,497,208.*

13 RW O'Brien, DW Cannon and WN Rowlands (1995), *Electroacoustic determination of particle size and zeta potential*, J. Colloid and Interface Science, 173: 406.

14 RW O'Brien (1990), *The electroacoustic equations for a colloidal suspension*, J. Fluid Mechanics, 212: 81.

15 RW O'Brien (1988), *Electroacoustic effects in a dilute suspension of colloidal particles*, J. Fluid Mechaics, 190: 71.

16 QD Nguyen and DV Boger (1983), *Yield stress measurement for concentrated suspensions*, J. Rheology, 27: 321.

17 QD Nguyen and DV Boger (1985), *Direct yield stress measurement with the vane technique*, J. Rheology, 29: 335.

18 CF Lockyear and MJD White (1979), *The WRC thickenability test using a low speed centrifuge: Technical Report TR118*, UK, Water Research Centre.

19 MD Green, M Eberl and KL Landman (1996), *Compressive yield stress of flocculated suspensions: Determination via experiment*, A.I.CH.E.J., in press.

20 PH King, HMM Koppers, C Vandermeyden, MWM van Eekeren and NC Wortel (1990), *Optimizing sludge characteristics and minimizing generation*, in Slib, Schlamm, Sludge, D.A. Cornwall and H.M.M. Koppers (Editors), American Water Works Association Research Foundation, Denver, USA, 47-108.

21 HL Neilson, KE Carns and JN DeBoice (1973), *Alum sludge thickening and disposal*, Journal AWWA, June: 385.

22 RJ Hunter (1987), *Foundations of Colloid Science, Vol I*, Oxford, UK, Clarendon Press.

23 JT Novak and N Bandak (1989), *Chemical conditioning and the resistance of sludges to shear*, Journal AWWA, March: 327.

24 RC Baskerville and RS Gale (1968), *A simple automatic technique for determining the filterability of sewage sludges*, Journal of the Institute of Water Pollution Control, 2: 3.

APPENDIX I

FERRIC CHLORIDE FLOCCULATION PROCESSES

The electrokinetics of a raw water model sludge consisting of silica and humics at pH 5.5 as a function of ferric chloride dose is shown in Figure A1. The data compares well with similar data using Al Cl_3 shown in Figure 15. Turbidity and colour data for the ferric chloride system are shown in Table A1.

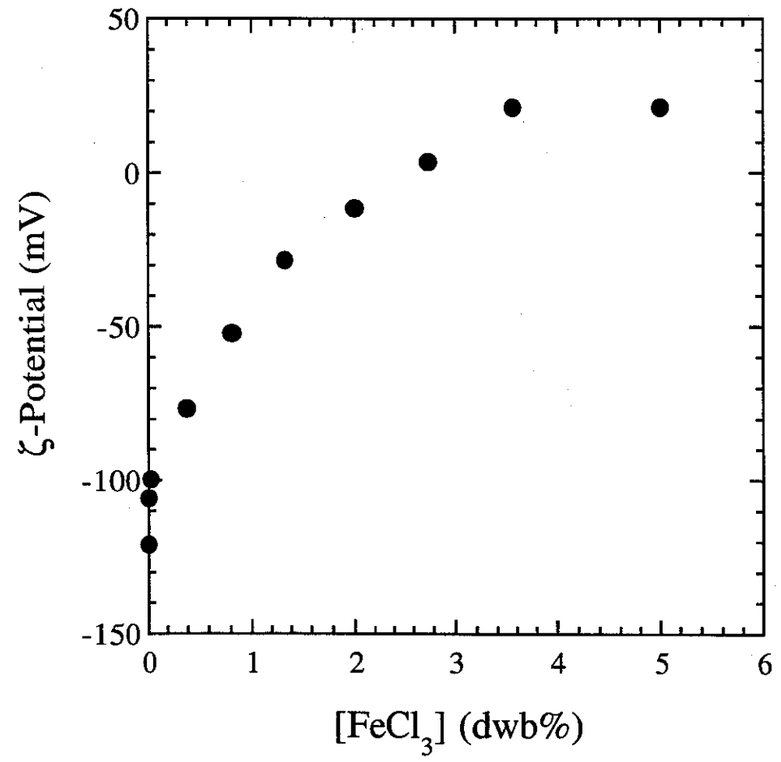

Figure A1 The zeta potential as a function of FeCl3 concentration at pH 5.5 for a 2.0 v/v % silica/humics model sludge.

Table A1 Physical properties of a model silica / humic acids sludge and its supernatant after conditioning with various $FeCl_3$ concentrations.

[$FeCl_3$] (dwb%)	Sludge Solids (v/v%)	Supernatant Colour (Pt - Co Units)	Supernatant Turbidity (NTU)
2.0	8.3	50	4.2
3.0	13.0	30	4.8
6.0	9.2	19	3.6

UWRAA RESEARCH REPORTS

Report Number	Title	Author
40	Community analysis of household water pressure satisfaction	G. J. Syme B. E. Nancarrow B. J. Bishop P. VanderWal
41	Assessment of coagulants for water treatment	C. Donati
42	Coagulants for water treatment: A generic guide	ACWQR
43	Optimal prices for urban water: A general equilibrium model applied to Melbourne	P.B. Dixon D.J. Baker
44	Applications of the Streaming Current Detector in water treatment	W. Barron D. R. Dixon M. Pascoe
45	Sydney coastal stormwater study	W. G. Rowlands et.al.
46	Identification of common noxious cyanobacteria: Part 2 – Chroococcales and Oscillatoriales	P. Baker
47	Levelling using the Global Positioning System	A. P. Armstrong P. A. Collier F. J. Leahy
48	Allocation of sewerage costs to customer segments	R. Hood P. Geary
49	Impact of urban lawns on nutrient contamination of an unconfined aquifer	M. L. Sharma D. E. Herne P. G. Kin J. D. M. Byrne
50	Early warning system for hazardous substances in sewage	R. O'Halloran B. A. Sexton N. H. Pilkington
51	Management model for trade waste discharges to small treatment plants (including PRELIM VERSION 4.0 Users Guide)	Camp Scott Furphy
52	Automatic meter reading: Link between meters and billing centre (Combined utilities trial)	B. Phey A. Leong Z. Balazic
53	Prediction of perceived odour strength and type from composition of sewage odour mixtures	D. G. Laing A. Eddy D. J. Best
54	Tracer studies using bacteriophage to predict the fate of viruses in the marine community: Preliminary assessments	B. J. Richardson A. L. Charlton S. Currie P. Ashton I. Lowther
55	Development of a water quality analyser suitable for unattended use in rivers and streams	G. W. Skyring I. A. Johns J. A. Cugley
56	Enhancement of nitrification in wastewater lagoons	P. M. Gross
57	Identification of critical water supply assets	PPK Consultants
58	Water in Our Environment: Education Project	H. Breidahl D. Cliffe H. Henderson
59	Electronic household water meter: Investigation into a cost effective design	Z. Balazic A. Leong
60	Domestic greywater reuse: Preliminary evaluation	B. Jeppesen
61	Chemical regeneration of activated carbon: A feasibility study	G. Newcombe
62	Tracing toxic discharges to sewers by analysis of biofilms (Stage 2)	W. H. Lock
63	Production of Jerusalem artichoke hybrids under irrigation using urban wastewater	M. Parameswaran
64	Control of pitting corrosion of copper tubes in potable waters	R. J. Taylor P. H. Cannington
65	Measurement of Total Factor Productivity in major water utilities: Melbourne case study	I. Manning E. Molyneux
66	Assimilable organic carbon as a measure of bacterial growth potential in water supplies	K. C. Tapang M. Drikas L. E. Bennett
67	Simultaneous peak water demands in residential areas	J. Henstridge G. J. Syme B. E. Nancarrow
68	Installation damage: Effect on lifetimes of uPVC pipes subjected to cyclic pressure	L. S. Burn
69	Safety aspects of the design of roadways as floodways	R. J. Keller B. Mitsch
70	Regional development implications of wastewater reuse: Werribee case study	D. Hunter W. Smith L. Nagy P. Jacob
71	Treatment of electroplating wastes using new-generation membrane technology	A. G. Fane Y. R. Shen
72	Stochastic economic approach to headworks augmentation timing	G. Kuczera W. S. Ng
73	Domestic greywater reuse: Overseas practice and its applicability to Australia	B. Jeppesen D. Solley
74	Decision support systems for the water industry: An Object-Oriented approach	J. M. Edwards
75	Chemical characterisation and olfactometric measurement of odours from sewage treatment process units	R. Kaye N. Mulhem D. Stone
76	Utilisation of sewage sludge for minesite rehabilitation: Rix's Creek Mine Trial	C. P. Phillips
77	A benchmarking methodology for the Australian water industry	I.R.C. Eggleton
78	Water quality effects of aeration/ destratification at Harding Reservoir, W.A.	R.S. Rosich T.A. McAuliffe

UWRAA RESEARCH REPORTS

Report Number	Title	Author
79	Heavy metals and organics in domestic wastewater	W. H. Lock
80	Effluent reuse: Land and wet weather storage requirement	J. M. Anderson T.J. Ruge
81	Graphical interactive pipe network analysis program	B.L. Berghout
82	Survey of pipeline rehabilitation techniques	Gutteridge Haskins & Davey
83	Bioavailability of aluminium from drinking water: Co-exposure with foods and beverages	J. Walton G. Hams D. Wilcox
84	Dezincification of brass in potable waters	D. Nicholas
85	Behaviour of aluminium during water treatment	P. Zhang M. McCormick J. Hughes M. Brymner
87	Benchmarking and best practice for urban waterway management	C. Aitken
88	Quantification of factors controlling the development of *Anabaena circinalis* blooms	J.A. Winder D.M.H. Cheng
89	Urban water, markets and the Hilmer reform process	R. Maddock N. Gonzalez
90	Remote sensing electronic device for hydrogen sulphide in the atmosphere	D.G. Laing D. Barnett G.G. Wallace
91	Simultaneous peak flows for medium density residential areas	J. Henstridge G.J. Syme B.E. Nancarrow S. Martens S. Gilbert
92	Die-off of human pathogens in stored wastewater sludge and sludge applied to land	R. Gibbs C. Hu G. Ho I. Unkovich P. Phillips
93	Benchmarking the economic performance of Australian urban water authorities	London Economics
94	Biological Nutrient Removal Plants: Review of Full-Scale Operation	K. Hartley
95	Stormwater Management in Australia: Community Perceptions, Attitudes and Knowledge	B E Nancarrow B S Jorgensen G J Syme
96	Development of a high resolution water quality model	Ch Zoppou S Roberts
97	Landfarming hydrocarbon wastes	W E Razzell P Griffin F Boevink
98	Water treatment plants for small communities	A B Roberts J A DeLaine
99	The role of biofilm and sediment accumulation and of chlorine tolerance in bacterial regrowth	K N Power R P Schneider K C Marshall
100	Phosphorus in Detergents: Its Contribution to Eutrophication in Australian Inland Waters	P Cullen A Heretakis A Herington
101	Disinfection of Wastewater Effluent: A Review of Current Techniques	C Hamilton
102	The effect of irrigation on Blue Gum (*Eucalyptus globulus)* water uptake	R H Froend G W Chester J K Marshall
103	Principles for Setting Developer's Contributions for Urban Water Infrastructure	G A Draper J F Thomas P B Mcleod
104	Epidemiological Evidence of Algal Toxins in Drinking Water and Recreational Waters	O El Saadi D A Steffensen
105	Detection of Cyanobacterial Peptide Toxins by a Non-Radioactive Protein Phosphatase Inhibition Assay	J F Wheldrake A Bilney L Rosenberg
107	Model Guidelines for Domestic Greywater Reuse for Australia	B Jeppesen
108	Advance Warning of Cyanobacterial Toxicity	A T R Sim J A P Rostas
109	Guidelines on the Quality of Stormwater and Treated Wastewater for Injection into Aquifers for Storage and Reuse	P Dillon P Pavelic
110	The Destruction of Cyanobacterial Peptide Toxins by Oxidants Used in Water Treatment	B Jeppesen
111	Application of Duckweed in Treating Municipal Wastewater	J Rositano
112	Alternative Overseas Water Treatment and Supply Practices	R A Leng
113	Ammonia Removal from Sirofloc® STP treated Sewage using Australian Natural Zeolite	N A Booker E L Cooney
114	Predicting the Failure Performance of Individual Water Mains	K Mavin

UWRAA RESEARCH REPORTS

Report Number	Title	Author
	Environmental Management Guidelines for the Australian Water Industry	S Mills
115	Drinking Water Disinfection By-Products Relevant to the 1996 NHMRC/ARMCANZ Guidelines	K L Simpson K P Hayes
119	Critical Evaluation of Domestic Irrigation Equipment	The Australian Irrigation Technology Centre

Report Number	Title	Author
	Other Reports	
200	Review of Drinking Water Treatment Coagulants	Gutteridge Haskins & Davey
201	Biological Aspects of Aluminium in Food and Water Supply	F Cumming
	Occasional Papers	
No 1	Water Pricing and the Marginal Cost of Water	R Warner
No 2	Systematic Environmental Management in the Water Industry: Toward Best Practice	S Mills